

國立臺灣大學理學院數學研究所

碩士論文

Department of Mathematics

College of Science

National Taiwan University

Master Thesis



兩分量玻色-愛因斯坦凝聚中孤立子碰撞的數值模擬
Numerical Simulations of Soliton Collisions in
Two-component Boes-Einstein Condensates

呂勇賢

Yung-Hsien Lu

指導教授：陳宜良博士

Advisor: I-Liang Chern, Ph.D.

中華民國 104 年 1 月

January, 2015





誌謝

我最感謝我的指導老師——陳宜良教授。這兩年來，陳老師教了我很多數學的知識及研究、寫作的方法。老師很博學，常常給出很棒的想法，拓展我的視野。老師也影響我很多，總是能感受到老師對各種問題的興趣和熱情，改變我面對很多事情的態度。謝謝老師在忙碌之餘仍然耐心地指導我，在適當的時候給予我鼓勵。

我要謝謝另外兩位口試委員鄧君豪教授及林太家教授。謝謝鄧老師去年熱心地幫助和教導。謝謝林老師在口試期間給予寶貴的建議。

我要謝謝我的家人、我的女朋友謝新誼、這些年來陪伴我的朋友謝沛剛、黃彥龍、黃志銘、楊秉澤、吳奐君。謝謝一起做研究的同學李柏毅、黃裕豪。謝謝研究室的好朋友曾膺任、邱詩凱、雷永裕、蕭煜修、石儲輔。

謝謝所有人對我的包容。





摘要

我們用數值方法來模擬在一維及二維空間兩分量玻色-愛因斯坦凝聚中二孤立子 (soliton) 的碰撞，探討孤立子在交互作用時速度和形狀的變化。我們用一個梯度下降法 [2](gradient flow method) 來計算二維空間中孤立子的形狀，以及利用時間分步正弦擬譜法 [1](time-splitting sine pseudospectral method) 來計算波函數隨時間的變化。數值模擬的結果顯示在一維空間中若孤立子間若有足夠強的相斥作用力，則它們的碰撞像是彈性碰撞；而在強相吸作用力下，孤立子在碰撞後將分為兩個或多個波包 (wave packets)。在二維空間中，孤立子間的相吸作用力如果夠強，則會在碰撞過程中發生爆破現象 (blow up phenomenon)，其它的情形下孤立子將在碰撞後成為漸漸散開 (spread out) 的波包。

關鍵字：兩分量、玻色-愛因斯坦凝聚、孤立子碰撞、數值模擬、變差等式、爆破。





Abstract

We investigate interaction of bright solitons for two-component Bose-Einstein condensates (BECs) in one and two dimensions numerically (1D, 2D). The numerical methods we adopt are: (1) Gradient flow with discrete normalization (GFDN) method for computing the profile function of solitons in 2D. We use backward Euler sine pseudospectral (BESP) method to discretize it. The algorithm is constructed by Chern and Bao [2]. (2) Time-splitting sine pseudospectral (TSSP) method for computing the evolution of wave functions. The algorithm is construct by Bao [1]. We discuss the change of velocities and shapes of the wave packets during and after the interactions between them. It is found that (1) In 1D, soliton collisions are like elastic collisions under strong repulsive interactions. When the interactions are attractive and strong enough, the wave packets may split into two or more parts after collisions. (2) In 2D, wave packets spread out after collisions when the interactions are repulsive or weak attractive. The wave functions blow up during interactions when the attractive interactions are strong enough.

Keywords: Two-component, Bose-Einstein condensates (BECs), Gross-Pitaevskii equation (GPE), Numerical simulations, Soliton collisions, Variance identity, Stability, Blow-up.





Contents

誌謝	iii
摘要	v
Abstract	vii
1 Introduction	1
2 Bright soliton solutions	7
2.1 Basic properties of solutions of GPE	7
2.2 Bright soliton solutions	13
2.3 Stability/Instability of solitons in 1D and 2D	18
3 Numerical methods	21
3.1 Gradient flow method for finding solitons in 2D	21
3.2 TSSP method for computing the dynamics of BECs	24
4 Numerical examples	31
4.1 Examples of one-component BEC: perturbations of solitons	31
4.2 Examples of two-component BECs: collisions of solitons	40
5 Conclusions	65
References	67

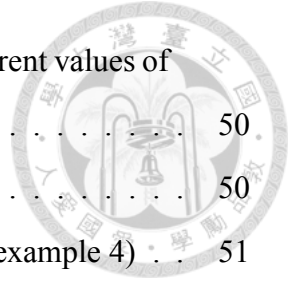




List of Figures

3.1	Soliton in 2D with $\ \phi\ _\infty = 1$	25
4.1	Density profile of $ \psi ^2$ at different time for $\epsilon = 0.01$	32
4.2	Difference vs. time graph for $\epsilon = 0.01$	33
4.3	Difference vs. time graph for $\epsilon = 0.001, 0.0001$	33
4.4	$ \psi(x) ^2$ at different time (case 1)	35
4.5	Energy vs. time graph (case 1)	36
4.6	w vs. time graph (case 1)	37
4.7	Density profile of the wave packet at different time (case 2)	38
4.8	$\ \psi\ _\infty^2$ vs. time graph (case 2)	38
4.9	Energy vs. time graph (case 2)	39
4.10	w vs. time graph (case 2)	39
4.11	Initial conditions in example 3	41
4.12	Density profiles of ψ_1 and ψ_2 at different time for $g_{12} = -2$ (example 3) .	42
4.13	Small waves separate from original solitons ($g_{12} = -5$)	43
4.14	Small waves separate from original solitons ($g_{12} = -9$)	43
4.15	Velocity v.s. time graph of soliton 1 and 2 with different values of g_{12} (example 3)	44
4.16	Density profiles of ψ_1 and ψ_2 at different time for $g_{12} = 0.1$ (example 3) .	45
4.17	Density profiles of ψ_1 and ψ_2 at different time for $g_{12} = 0.95$ (example 3)	46
4.18	Density profiles of ψ_1 and ψ_2 at different time for $g_{12} = 5$ (example 3) . .	47
4.19	Velocity v.s. time graph for different values of g_{12} (example 3)	49

4.20	Velocities of the two wave packets after collisions with different values of g_{12} (example 3)	50
4.21	Initial conditions in example 4	50
4.22	Density profiles of ψ_1 and ψ_2 at different time for $g_{12} = 2$ (example 4)	51
4.23	Density profiles of ψ_1 and ψ_2 at different time for $g_{12} = 4$ (example 4)	53
4.24	Density profiles of ψ_1 and ψ_2 at different time for $g_{12} = 6$ (example 4)	54
4.25	$ \langle v \rangle $ v.s. time with different values of g_{12} (example 4)	55
4.26	w v.s. time graph after collision for $g_{12} = 2$ (example 4)	56
4.27	Density profiles of ψ_1 and ψ_2 at different time for $g_{12} = -1$ (example 4)	57
4.28	$ d\langle x \rangle_1/dt $ v.s. time with different values of g_{12} (example 4)	58
4.29	Density profiles of ψ_1 and ψ_2 at different time for $g_{12} = -6$ (example 4)	60
4.30	Density profiles of ψ_1 and ψ_2 at different time for $g_{12} = -6$ (2) (example 4)	61
4.31	Energy v.s. time graph for $g_{12} = -6$	62
4.32	Density profiles of ψ_1 and ψ_2 at different time for $g_{12} = -8$ (example 4)	63
4.33	Energy v.s. time graph for $g_{12} = -8$ (example 4)	64





List of Tables

3.1	Errors for $\tau = 1/1024$ and various values of h (case 1)	28
3.2	Errors for $h = 1/16$ and various values of τ (case 1)	28
3.3	Errors for $h = 1/16$ and various values of τ (case 2)	29
3.4	Errors for $h = 1/16$ and various values of τ (case 3)	30





1. Introduction

What are BECs

Bose-Einstein condensation is a phenomenon originally predicted by Bose and Einstein in 1924, and was first realized after 70 years in 1995. When a dilute boson gas is cooled to extremely low temperature (below a 10^{-7} K), the interaction between bosons are weak, and large number of bosons occupy the same quantum state. This gas is called a Bose-Einstein condensate (BEC). The realization of BECs makes the quantum effects become apparent at a macroscopic scale.

Mathematical model - Gross-Pitaevskii equation

In quantum mechanics, the evolution of a single particle is described by the time-dependent Schrödinger equation

$$i\hbar\frac{\partial}{\partial t}\psi(x, t) = H\psi(x, t),$$

where ψ is the state function, \hbar is the reduced Planck constant and H is the Hamiltonian. The Hamiltonian for a single particle is of the form

$$H_s\psi_s(x, t) = \left(-\frac{\hbar^2}{2m}\nabla^2 + V(x) \right) \psi_s(x, t).$$

where m is the mass of the particle, $V(x)$ is the applied potential. The BEC is a dilute ultra cold gas. It is a many particle system. The interaction between particles has to be taken into account. We consider the binary interaction between particles. We denote the interacting potential between particle i and j by $V_{int}(|x_i - x_j|)$, where x_i, x_j are the

positions of particle i, j , respectively. The many-body Hamiltonian of the system takes the form

$$H_N = \left(-\frac{\hbar^2}{2m} \sum_{1 \leq i \leq N} \nabla_i^2 + V_{ext}(x_i) \right) + \sum_{1 \leq i < j \leq N} V_{int}(|x_i - x_j|),$$

where V_{ext} is the external trapping potential. By the mean field theory [5], the interacting potential is approximated by

$$V_{int}(|x_i - x_j|) \approx g\delta(|x_i - x_j|),$$

where δ is the Dirac delta function, g is the coefficient representing the strength of inter-particle interactions (negative for attractive interactions and positive for repulsive interactions). In BECs we expect all the particles (bosons) occupying the ground state, thus we take the Hartree ansatz for the many-body wave function

$$\psi_N(x_1, x_2, \dots, x_N, t) = \prod_{i=1}^N \psi_s(x_i, t).$$

Each is normalized with $\int |\psi_s(x)|^2 dx = 1$.

By a formal calculation, the energy of ψ_N is

$$E(\psi_N) = N \int_{\mathbb{R}^3} \left[\frac{\hbar^2}{2m} |\nabla \psi_s(x, t)|^2 + V_{ext}(x) |\psi_s(x, t)|^2 + \frac{N-1}{2} g |\psi_s(x, t)|^4 \right] dx. \quad (1.1)$$

Now let us introduce the wave function

$$\psi(x, t) = \sqrt{N} \psi_s$$

for the whole condensate. Then we have

$$N = \int |\psi(x, t)|^2 dx,$$

and we define the energy of ψ as

$$E(\psi) = \int_{\mathbb{R}^3} \left[\frac{\hbar^2}{2m} |\nabla \psi(x, t)|^2 + V_{ext}(x) |\psi(x, t)|^2 + \frac{g}{2} |\psi(x, t)|^4 \right] dx \approx E(\psi_N).$$



Each term corresponds to the kinetic energy, the potential energy and the interaction energy, respectively. Minimizing this energy with respect to infinitesimal variations in ψ^* , the complex conjugate of ψ , we get the Hamiltonian in the form

$$H\psi = \frac{\delta E}{\delta \psi^*} = \left[-\frac{\hbar^2}{2m} \nabla^2 + V_{ext}(x) + g|\psi(x, t)|^2 \right] \psi(x, t).$$

The time-evolution of BECs is described by the time-dependent Schrödinger equation, which is

$$i\hbar \frac{\partial}{\partial t} \psi(x, t) = \left[-\frac{\hbar^2}{2m} \nabla^2 + V_{ext}(x) + g|\psi(x, t)|^2 \right] \psi(x, t), \quad x \in \mathbb{R}^3, t > 0.$$

This equation is also known as the Gross-Pitaevskii equation (GPE).

In experiments, mixtures of different species of condensates have been created. Multi-component BECs can be described by a system of coupled Gross-Pitaevskii equations (CGPEs)

$$i\hbar \frac{\partial}{\partial t} \psi_k = -\frac{\hbar^2}{2m_k} \nabla^2 \psi_k + V_{ext,k}(x) \psi_k + \sum_{l=1}^{\mathcal{N}} g_{kl} |\psi_l|^2 \psi_k,$$

where ψ_k is the k th component wave function ($k = 1, 2, \dots, \mathcal{N}$), m_k is the mass of the particle in k th component, V_k is the potential confining the k th component, and g_{kl} is the interaction coefficient representative the interaction between the k th and the l th components ($g_{kl} = g_{lk}$).

Soliton solutions

The complex wave function $\psi(x, t)$ of a single species BEC can be expressed in terms of the density $\rho(x, t) \equiv |\psi(x, t)|^2$ and phase $S(x, t)$ as

$$\psi(x, t) = \sqrt{\rho(x, t)} e^{iS(x, t)}.$$

The current density j is defined as

$$j \equiv \frac{\hbar}{2mi} (\psi^* \nabla \psi - \psi \nabla \psi^*) = \rho v,$$

where v is the atomic velocity. Thus we have

$$v(x, t) = \frac{\hbar}{m} \nabla S(x, t),$$

means that the gradient of the phase is the atomic velocity.

When the external potential $V_{ext} = 0$, the GPE possesses solutions of the form

$$\psi(x, t) = \phi(x - vt) e^{iS(x,t)},$$

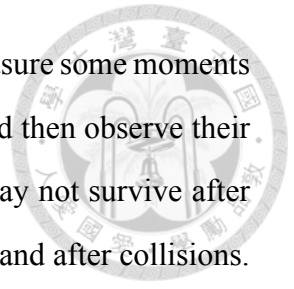
where ϕ are real functions describe the shape of the condensates and v is constant here. Solutions of this form are called soliton solutions, the kinetic and interaction energy of them are balanced so the waves can travel without change of shapes. We focus on the solitons which are localized in space (decay as x goes to infinity). Notice that the GPE (without external potential) possesses this type of soliton solutions only when the interaction coefficient g is negative, means that the interaction between atoms are attractive. Solitons are stable in one-dimension (1D) and unstable in two- and three- dimensions (2D, 3D). In 1D, according to the soliton resolution conjecture [12], the solutions should eventually resolve into a finite number of solitons, plus dispersive waves which decays to zero. In 2D and 3D, perturbations of solitons may cause the solutions blow up in a finite time or disperse to infinity [11].

Goal

In this paper, we take the external potential $V_{ext} = 0$ and discuss the results of interactions between solitons. We investigate evolutions of two colliding solitons in 1D and 2D by numerical methods.



In 1D, solitons are stable and they can survive after collisions. We measure some moments of the waves such as center of mass, speed of center of mass, etc., and then observe their variations during the collisions. In 2D, solitons are unstable, they may not survive after collisions. We solve the CGPEs to see how the waves change during and after collisions.







2. Bright soliton solutions

In this section we review some properties of solutions of GPE and then introduce the bright soliton solutions. We rescale the GPE in the unit $\hbar = m = 1$ for convenience:

$$i\frac{\partial}{\partial t}\psi(x, t) = -\frac{1}{2}\nabla\psi(x, t) + V_{ext}(x)\psi(x, t) + g|\psi|^2\psi(x, t). \quad (2.1)$$

2.1 Basic properties of solutions of GPE

Invariants

Let $\psi(x, t)$ be a solution of (2.1). There exist two invariants with respect to time. One is the total number of atoms (or the total mass since we let the mass of the atom $m = 1$).

$$N(\psi(x, t)) = \int_{\mathbb{R}^d} |\psi(x, t)|^2 dx \equiv \int_{\mathbb{R}^d} |\psi(x, 0)|^2 dx = N(\psi(x, 0)),$$

and the other is the energy

$$\begin{aligned} E(\psi(x, t)) &= \int_{\mathbb{R}^d} \left[\frac{1}{2} |\nabla\psi(x, t)|^2 + V_{ext}(x)|\psi(x, t)|^2 + \frac{g}{2} |\psi(x, t)|^4 \right] dx \\ &\equiv \int_{\mathbb{R}^d} \left[\frac{1}{2} |\nabla\psi(x, 0)|^2 + V_{ext}(x)|\psi(x, 0)|^2 + \frac{g}{2} |\psi(x, 0)|^4 \right] dx = E(\psi(x, 0)). \end{aligned}$$

The invariance of the total mass is obtained by multiplying GPE by ψ^* and taking the imaginary part, and the invariance of the energy is obtained by multiplying GPE by $d\psi^*/dt$ and taking the real part. In fact, for one-dimensional cubic nonlinear Schrodinger equation, there are infinitely many invariants. It is an integrable system. But here, we are only

interested in the basic two invariants, the mass and the total energy, which is related to the classical mechanics directly.

For coupled GPEs we have similar results (obtained by similar techniques). The mass and total energy are also invariant in time:

$$N_i(t) = \int_{\mathbb{R}^d} |\psi_i(x, t)|^2 dx \equiv \int_{\mathbb{R}^d} |\psi_i(x, 0)|^2 dx = N_i(0),$$

$$\begin{aligned} E_{total} &= \sum_{i=1}^{\mathcal{N}} E_i(t) \\ &= \sum_{i=1}^{\mathcal{N}} \int_{\mathbb{R}^d} \left[\frac{1}{2} |\nabla \psi_i(x, t)|^2 + \sum_{j=1}^{\mathcal{N}} \frac{g_{ij}}{2} |\psi_j(x, t)|^2 |\psi_i(x, t)|^2 \right] dx \\ &\equiv \sum_{i=1}^{\mathcal{N}} \int_{\mathbb{R}^d} \left[\frac{1}{2} |\nabla \psi_i(x, 0)|^2 + \sum_{j=1}^{\mathcal{N}} \frac{g_{ij}}{2} |\psi_j(x, 0)|^2 |\psi_i(x, 0)|^2 \right] dx \\ &= \sum_{i=1}^{\mathcal{N}} E_i(0). \end{aligned}$$

Moments

A useful tool for analysing BEC dynamics is the moment method [3]. Moments of a wave function are expected values of physical quantities of atoms in the condensate. They provide physical properties of condensates in a macroscopic scale. The total mass is the zeroth moment of the density function

$$N = \int_{\mathbb{R}^d} \rho dx = \int_{\mathbb{R}^d} |\psi|^2 dx.$$

The center of mass is the first moment divided by the total mass

$$\langle x \rangle = \frac{1}{N} \int_{\mathbb{R}^d} x \rho dx = \frac{1}{N} \int_{\mathbb{R}^d} x |\psi|^2 dx.$$

The variance is the second moment

$$\mathcal{V} = \int_{\mathbb{R}^d} |x|^2 \rho dx = \int_{\mathbb{R}^d} |x|^2 |\psi|^2 dx.$$



The center of velocity

$$\langle v \rangle = \frac{1}{N} \int_{\mathbb{R}^d} v \rho dx = \frac{1}{N} \int_{\mathbb{R}^d} \frac{1}{2i} (\psi^* \nabla \psi - \psi \nabla \psi^*) dx.$$

The center of velocity gives the velocity of the whole condensate, we have the equality

$$\langle v \rangle = \frac{d\langle x \rangle}{dt}.$$

We also have the equation describing the time evolution of $\langle v \rangle$

$$\frac{d\langle v \rangle}{dt} = \langle -\nabla V_{ext} \rangle = \frac{1}{N} \int_{\mathbb{R}^d} -|\psi|^2 \nabla V_{ext} dx.$$

This equation tells us that the interaction between atoms play no role in time evolution of $\langle v \rangle$, the change of velocity in time only depends on the gradient of potential.

Variance identity

Variance identity can help us analysing the stability of a soliton [8]. By the variance identity, we get that wave packets in 2D with negative energy blow up in a finite time. As mentioned above, the variance is defined as

$$\mathcal{V} = \int_{\mathbb{R}^d} |x|^2 |\psi|^2 dx,$$

which is the second moment of the density function $|\psi|^2$. Since the center of mass of a condensate is not necessarily at the origin, we define the second moment of $|\psi|^2$ about the center of mass as the width of the wave packet w :

$$w = \int_{\mathbb{R}^d} |x - \langle x \rangle|^2 |\psi|^2 dx = \int_{\mathbb{R}^d} (|x|^2 - |\langle x \rangle|^2) |\psi|^2 dx, \quad (2.2)$$

We will identify whether a wave packet blows up or spreads out by finding w as a function of time. If the width of the wave packet w goes to zero in finite time, then we know the wave packet blows up; if w goes to infinity as time goes to infinity, then the wave packet eventually spreads out.

Now we give the variance identity, and we will give the proof later:

$$\frac{d^2\mathcal{V}}{dt^2} = 4E + g(d-2) \int_{\mathbb{R}^d} |\psi|^4 dx, \quad (2.3)$$

where d is the dimension of the space. In 2D, the above equation can be simplified to

$$\mathcal{V}(t) = 2Et^2 + \frac{d\mathcal{V}}{dt}(0)t + \mathcal{V}(0). \quad (2.4)$$

Since the energy is conserved, this equation tells us that we can directly get the variance of a solution at any time with a given initial condition in 2D.

The width of a wave packet w is related to \mathcal{V} by the equality

$$w = \mathcal{V} - N|\langle x \rangle|^2.$$

If we set the external potential $V_{ext} = 0$, then the center of mass $\langle x \rangle = \langle v \rangle t + x_0$, where the velocity $\langle v \rangle$ is constant and x_0 is the center of mass at $t = 0$. Hence we have

$$\begin{aligned} w(t) &= 2Et^2 + \frac{d\mathcal{V}}{dt}(0)t + \mathcal{V}(0) - N|\langle v \rangle t + x_0|^2 \\ &= 2 \left(E - \frac{1}{2}N|\langle v \rangle|^2 \right) t^2 + \left(\frac{d\mathcal{V}}{dt}(0) - 2N\langle v \rangle \cdot x_0 \right) t + \mathcal{V}(0) - N|x_0|^2. \end{aligned}$$

For convenience we define the internal kinetic energy as the energy minus the kinetic energy for center of mass

$$KE_{int} = E - \frac{1}{2}N|\langle v \rangle|^2.$$

Thus, we get that if the internal kinetic energy of a solution is negative, then the width of the solution tends to zero in finite time, and hence the solution blows up. If E' of a solution is positive, then the width of the wave packet tends to infinity as time goes to

infinity, and hence the solution may eventually be a dispersive wave.



Proof of the variance identity (2.3)

Here we give the proof of the variance identity, it is from [8]. We first multiply the single Gross-Pitaevskii equation

$$i\psi_t = -\frac{1}{2}\Delta\psi + g|\psi|^2\psi$$

by ψ^* and take the imaginary part. Then we obtain

$$i(\psi^*\psi_t + \psi\psi_t^*) = \frac{1}{2}((\Delta\psi^*)\psi - (\Delta\psi)\psi^*).$$

Thus we have

$$\frac{\partial}{\partial t}|\psi|^2 = -\frac{i}{2}((\Delta\psi^*)\psi - (\Delta\psi)\psi^*) = \text{Im}((\Delta\psi^*)\psi),$$

and it can be reduced to

$$\frac{\partial}{\partial t}|\psi|^2 = \nabla \cdot (\text{Im}(\psi\nabla\psi^*)). \quad (2.5)$$

Multiply the above equation by $|x|^2$ and integrate over \mathbb{R}^d , we get

$$\int_{\mathbb{R}^d} |x|^2 \frac{\partial}{\partial t} |\psi|^2 dx = - \int_{\mathbb{R}^d} (\nabla |x|^2) \cdot \text{Im}(\psi\nabla\psi^*) dx = -2 \int_{\mathbb{R}^d} x \cdot \text{Im}(\psi\nabla\psi^*) dx. \quad (2.6)$$

Next we multiply the single GPE by $x \cdot \nabla\psi^*$ and integrate the real part over \mathbb{R}^d , then we get

$$I = II + III, \quad (2.7)$$

where

$$I = i \int_{\mathbb{R}^d} (x \cdot \nabla\psi^*) \psi_t - (x \cdot \nabla\psi) \psi_t^* dx \quad (2.8)$$

$$II = -\frac{1}{2} \int_{\mathbb{R}^d} (x \cdot \nabla\psi^*) \Delta\psi + (x \cdot \nabla\psi) \Delta\psi^* dx \quad (2.9)$$

$$III = g \int_{\mathbb{R}^d} |\psi|^2 \psi (x \cdot \nabla\psi^*) + |\psi|^2 \psi^* (x \cdot \nabla\psi) dx \quad (2.10)$$

We integrate equation (2.9) and (2.10) by parts and obtain



$$\begin{aligned}
II &= \frac{1}{2} \int_{\mathbb{R}^d} \sum_{j=1}^d \left(\frac{\partial}{\partial x_j} \psi^* \right) \left(\frac{\partial}{\partial x_j} \psi \right) + \sum_{j=1}^d \sum_{i=1}^d x_i \left(\frac{\partial}{\partial x_i} \frac{\partial}{\partial x_j} \psi^* \right) \left(\frac{\partial}{\partial x_j} \psi \right) \\
&\quad + \sum_{j=1}^d \left(\frac{\partial}{\partial x_j} \psi \right) \left(\frac{\partial}{\partial x_j} \psi^* \right) + \sum_{j=1}^d \sum_{i=1}^d x_i \left(\frac{\partial}{\partial x_i} \frac{\partial}{\partial x_j} \psi \right) \left(\frac{\partial}{\partial x_j} \psi^* \right) dx \\
&= \frac{1}{2} \int_{\mathbb{R}^d} 2|\nabla \psi|^2 + \sum_{j=1}^d \sum_{i=1}^d x_i \frac{\partial}{\partial x_i} \left(\frac{\partial}{\partial x_j} \psi \right) dx \\
&= \frac{1}{2} \int_{\mathbb{R}^d} 2|\nabla \psi|^2 + x \cdot \nabla (|\nabla \psi|^2) dx \\
&= \frac{1}{2} \int_{\mathbb{R}^d} 2|\nabla \psi|^2 + d (|\nabla \psi|^2) dx \\
&= (2-d) \int_{\mathbb{R}^d} \frac{1}{2} |\nabla \psi|^2 dx,
\end{aligned}$$

$$\begin{aligned}
III &= g \int_{\mathbb{R}^d} |\psi|^2 \psi (x \cdot \nabla \psi^*) + |\psi|^2 \psi^* (x \cdot \nabla \psi) dx \\
&= g \int_{\mathbb{R}^d} -[\nabla \cdot (|\psi|^2 \psi x)] \psi^* + |\psi|^2 \psi^* (x \cdot \nabla \psi) dx \\
&= -g \int_{\mathbb{R}^d} \nabla \psi^* \cdot (|\psi|^2 \psi x) + \nabla \psi \cdot (|\psi|^2 \psi^* x) + d (|\psi|^4) dx \\
&= -III - gd \int_{\mathbb{R}^d} |\psi|^4 dx.
\end{aligned}$$

So we have

$$II = (2-d) \int_{\mathbb{R}^d} \frac{1}{2} |\nabla \psi|^2 dx, \quad (2.11)$$

$$III = -\frac{gd}{2} \int_{\mathbb{R}^d} |\psi|^4 dx. \quad (2.12)$$

Now by equation (2.6) to equation (2.12), we have



$$\begin{aligned}
\frac{d^2}{dt^2} \mathcal{V} &= -2 \frac{d^2}{dt^2} \int_{\mathbb{R}^d} x \cdot \text{Im}(\psi \nabla \psi^*) dx \\
&= -2 \frac{d^2}{dt^2} \int_{\mathbb{R}^d} \frac{-i}{2} ((x \cdot \nabla \psi^*) \psi - (x \cdot \nabla \psi) \psi^*) dx \\
&= i \int_{\mathbb{R}^d} (x \cdot \nabla \psi_t^*) \psi + (x \cdot \nabla \psi^*) \psi_t - (x \cdot \nabla \psi_t) \psi^* - (x \cdot \nabla \psi) \psi_t^* dx \\
&= I + i \int_{\mathbb{R}^d} (x \cdot \nabla \psi_t^*) \psi - (x \cdot \nabla \psi_t) \psi^* dx \\
&= I + i \int_{\mathbb{R}^d} (\nabla \cdot (\psi^* x)) \psi_t - (\nabla \cdot (\psi x)) \psi_t^* dx \\
&= I + i \int_{\mathbb{R}^d} [(x \cdot \nabla \psi^*) \psi_t - (x \cdot \nabla \psi) \psi_t^*] + d(\psi^* \psi_t - \psi \psi_t^*) dx \\
&= 2I + d \int_{\mathbb{R}^d} \psi^* (i \psi_t) + \psi (-i \psi_t^*) dx \\
&= 2I + d \int_{\mathbb{R}^d} |\nabla \psi|^2 + 2g|\psi|^4 dx \\
&= (4 - 2d) \int_{\mathbb{R}^d} \frac{1}{2} |\nabla \psi|^2 dx - gd \int_{\mathbb{R}^d} |\psi|^4 dx \\
&+ 2d \int_{\mathbb{R}^d} \frac{1}{2} |\nabla \psi|^2 dx + 2gd \int_{\mathbb{R}^d} |\psi|^4 dx \\
&= 4 \int_{\mathbb{R}^d} \frac{1}{2} |\nabla \psi|^2 dx + gd \int_{\mathbb{R}^d} |\psi|^4 dx \\
&= 4 \int_{\mathbb{R}^d} \frac{1}{2} |\nabla \psi|^2 + \frac{g}{2} |\psi|^4 dx + g(d - 2) \int_{\mathbb{R}^d} |\psi|^4 dx \\
&= 4E + g(d - 2) \int_{\mathbb{R}^d} |\psi|^4 dx.
\end{aligned}$$

Thus we completes the proof.

2.2 Bright soliton solutions

Without the trapping potential V_{ext} , GPE possesses bright soliton solutions when the interaction coefficient $g < 0$ (focusing). Bright solitons are travelling waves which decay at infinity in space. They travel at a constant velocity without change of shape.

As mentioned in section 1, soliton solutions can be written in the form

$$\psi(x, t) = \phi(x - vt) e^{iS(x, t)}.$$

We call ϕ the shape function of the soliton. The shape function of solitons in 1D are hyperbolic secant functions. The shape functions of solitons in high space dimensions satisfy a nonlinear elliptic equation which can be solved numerically. The phase function $S(x, t)$ is correlated with the shape function ϕ and the velocity v of the soliton.

We first find the soliton solutions in 1D, then discuss the general form in multi-dimensional space.

Soliton solutions in 1D

This process of finding soliton solutions in 1D is very similar to the process in chapter 4 of [6]. When the potential $V_{ext} = 0$ and $g = -1$, the GPE becomes

$$i \frac{\partial}{\partial t} \psi = -\frac{1}{2} \Delta \psi - |\psi|^2 \psi. \quad (2.13)$$

The soliton wave solution in 1D assumes the form

$$\psi(x, t) = \phi(x - vt) e^{i(kx - \omega t)} = \phi(\xi) e^{i(kx - \omega t)}, \quad (2.14)$$

where ϕ is real, v , k , and ω are the group velocity, wave number and frequency, respectively. The function ϕ is assumed to be 0 at $x = \pm\infty$. Substituting (2.14) into (2.13), we have

$$\begin{aligned} i \frac{\partial}{\partial t} \psi &= -iv\phi' e^{i(kx - \omega t)} + \omega\phi e^{i(kx - \omega t)} \\ -\frac{1}{2} \frac{\partial^2}{\partial x^2} \psi &= -\frac{1}{2} \phi'' e^{i(kx - \omega t)} - ik\phi' e^{i(kx - \omega t)} + \frac{1}{2} k^2 \phi e^{i(kx - \omega t)} \\ -|\psi|^2 \psi &= -|\phi|^2 \phi e^{i(kx - \omega t)}, \end{aligned}$$

thus equation (2.13) becomes

$$\frac{1}{2} \phi'' e^{i(kx - \omega t)} = -i(k - v)\phi' e^{i(kx - \omega t)} - \left(\omega - \frac{k^2}{2}\right) \phi e^{i(kx - \omega t)} - |\phi|^2 \phi e^{i(kx - \omega t)}.$$



Choose $v = k$ and divide by $e^{i(kx-\omega t)}$, we obtain

$$\frac{1}{2}\phi'' = -\left(\omega - \frac{k^2}{2}\right)\phi - \phi^3.$$

Multiply this equality by ϕ'

$$\frac{1}{2}\phi''\phi' = -\left(\omega - \frac{k^2}{2}\right)\phi\phi' - \phi^3\phi',$$

then integrate both sides and we get

$$\frac{1}{4}(\phi')^2 = -\frac{1}{2}\left(\omega - \frac{k^2}{2}\right)\phi^2 - \frac{1}{4}\phi^4 + c_1.$$

We assume $\phi, \phi' \rightarrow 0$ as $\xi \rightarrow \pm\infty$, so that $c_1 = 0$. Hence

$$\phi' = \pm\phi\sqrt{(k^2 - 2\omega) - \phi^2}.$$

We take the minus sign, and use the implicit formula for ϕ :

$$\xi = -\int_0^{\phi(\xi)} \frac{dy}{y\sqrt{(k^2 - 2\omega) - y^2}} + c_2.$$

Choose $c_2 = 0$ and substitute $y = \sqrt{k^2 - 2\omega} \operatorname{sech} \theta$, then we have

$$\begin{aligned} y^2 &= (k^2 - 2\omega) \operatorname{sech}^2 \theta \\ dy &= -\sqrt{k^2 - 2\omega} \operatorname{sech} \theta \tanh \theta d\theta \\ y\sqrt{(k^2 - 2\omega) - y^2} &= \sqrt{k^2 - 2\omega} \operatorname{sech} \theta \sqrt{(k^2 - \omega)} \tanh \theta. \end{aligned}$$

Hence

$$\xi = \int_0^{\phi(\xi)} \frac{1}{\sqrt{k^2 - 2\omega}} d\theta.$$

Let $\sqrt{k^2 - 2\omega} = \eta$, then

$$\xi = \frac{\theta}{\eta}.$$

So $\theta = \eta\xi$, $\phi(\xi) = \eta \operatorname{sech}(\eta\xi)$, and finally we get the bright soliton solutions in 1D:

$$\psi(x, t) = \eta \operatorname{sech}(\eta(x - vt)) e^{i(kx - \omega t)},$$

where the dispersion relation is

$$\omega = \frac{1}{2} (k^2 - \eta^2).$$

We express the soliton solutions in the form $\psi(x, t) = \sqrt{\rho} e^{iS}$. The particle density of the bright soliton is $\eta^2 \operatorname{sech}^2(\eta(x - vt))$, which is localized within a small region with width η , and travelling at speed v . On the other hand, the velocity of the soliton is $\nabla S = k = v$, agree with our assumption.

General form of soliton solutions in d-dimension

In fact, the shape function of a bright soliton ϕ is a bound state defined as follows. We consider a stationary solution in d-dimension

$$\psi(x, t) = \phi(x) e^{-i\mu t}, \quad x \in \mathbb{R}^d,$$

where μ is the chemical potential of the condensate. Then we plug it into the GPE (with $V_{ext} = 0$), the shape function ϕ satisfies the time-independent GPE

$$\mu\phi = -\frac{1}{2}\Delta\phi + g|\phi|^2\phi.$$

We rewrite this equation as

$$-\frac{1}{2}\Delta\phi - \mu\phi + g|\phi|^2\phi = 0. \quad (2.15)$$

When the interaction coefficient $g < 0$ and $\mu < 0$, there exist nontrivial solutions to equation (2.15) which decays at infinity [9]. Let ϕ be such a solution, then we call it a



bound state associate with μ . Then bright soliton solutions are wave functions of the form

$$\psi(x, t) = \phi(x - vt - x_0) e^{i(v \cdot x - \frac{|v|^2}{2}t - \mu t - \delta_0)}$$



which describes a solitary wave travelling with velocity v . However, in this paper we just focus on those solitons whose shape function is a ground state. A ground state is a bound state which minimizes the action

$$S(\phi) = \int_{\mathbb{R}^d} \frac{1}{4} |\nabla \phi|^2 - \frac{\mu}{2} |\phi|^2 + \frac{g}{4} |\phi|^4 dx.$$

In fact, it can be proven that for fixed μ the ground state solution is the unique solution which is positive and radially symmetric [9]. We denote the ground state associated to μ by ϕ_μ . Then the (ground state) solitons are of the form

$$\psi(x, t) = \phi_\mu(x - vt - x_0) e^{i(v \cdot x - \frac{|v|^2}{2}t - \mu t - \delta_0)}.$$

Notice that the velocity does not depend on ϕ_μ . We can choose the velocity of a soliton as initial conditions once we have the ground state ϕ_μ .

The ground state associated to different values of μ can be obtained by scaling. Consider a positive wave function ϕ_μ satisfies the time-independent GPE

$$-\frac{1}{2} \Delta \phi_\mu - \mu \phi_\mu + g |\phi_\mu|^2 \phi_\mu = 0.$$

Multiply the above equation by η^3 and replace x by y , we obtain

$$-\frac{1}{2} \eta^3 \Delta_y \phi_\mu(y) - \eta^3 \mu \phi_\mu(y) + \eta^3 g |\phi_\mu(y)|^2 \phi_\mu(y) = 0.$$

Let $y = \eta x$, we have

$$-\frac{1}{2} \Delta_x (\eta \phi_\mu(\eta x)) - \eta^2 \mu (\eta \phi_\mu(\eta x)) + g |\eta \phi_\mu(\eta x)|^2 (\eta \phi_\mu(\eta x)) = 0.$$



Then choose $\phi_{\mu'}(x) = \eta\phi_{\mu}(\eta x)$, we get

$$-\frac{1}{2}\Delta\phi_{\mu'} - \mu'\phi_{\mu'} + g|\phi_{\mu'}|^2\phi_{\mu'} = 0,$$

where $\mu' = \eta^2\mu$. Hence $\phi_{\mu'}$ also satisfies the time-independent GPE. This tells us that once we have a ground state ϕ_{μ} with some chemical potential μ , we can get all other ground states by rescaling ϕ_{μ} .

Notice that this kind of scaling doesn't change the 2-norm of the wave functions in 2D, and hence we know that all ground states (with different values of μ) in 2D are of the same mass.

2.3 Stability/Instability of solitons in 1D and 2D

In this section we review some theorems about the global existence of the solution and the stability of ground state solitons in 1D and 2D.

Existence of solutions

Two dimension is the critical dimension for existing solutions blow up in a finite time. We give a theorem which states a sharp sufficient condition for global existence, from [13].

Theorem 1. *Let $\varphi \in H^1(\mathbb{R}^d)$. For dimension $d = 2$, a sufficient condition for global existence (the solution exist for all time) for the initial-value problem*

$$i\frac{\partial}{\partial t}\psi(x, t) = -\frac{1}{2}\Delta\psi(x, t) + g|\psi|^2\psi(x, t), \quad x \in \mathbb{R}^d, t \in \mathbb{R}^+, \quad (2.16)$$

$$\psi(x, 0) = \varphi(x), \quad x \in \mathbb{R}^d, \quad (2.17)$$

is:

$$\|\varphi\|_{L^2}^2 < \|\phi\|_{L^2}^2.$$

Here ϕ is a positive ground state solution of the time-independent GPE (2.15).

This theorem tells us that a solution in 2D may blow up only when its mass is greater

than or equal to the mass of a soliton.



Stability/Instability of solitons

We give two theorems about the stability/instability of solitons in 1D and 2D, respectively.

Theorem 2 (Orbital stability in 1D [4]). *In 1D, let ϕ be the ground state of the time-independent GPE (2.15). Then for any $\epsilon > 0$, there exist $\delta > 0$ such that if the initial condition φ obeys*

$$\inf_{\theta \in \mathbb{R}, y \in \mathbb{R}^d} |\varphi(\cdot) - e^{i\theta} \phi(\cdot + y)|_{H^1} < \delta,$$

then the solution $\psi(x, t)$ of the initial value problem (2.16)-(2.17) satisfies

$$\inf_{\theta \in \mathbb{R}, y \in \mathbb{R}^d} |\psi(x, \cdot) - e^{i\theta} \phi(\cdot + y)|_{H^1} < \epsilon.$$

The orbit of a function u is defined as

$$\mathcal{G}_u = \{u(\cdot + x_0)e^{i\gamma}, \forall x_0 \in \mathbb{R}^d, \gamma \in [0, 2\pi)\}.$$

This theorem tells us that if the initial condition φ is close to a ground state ϕ in H^1 norm, up to the transformations keeping the equation invariant (translation and phase shift), then the solution ψ at any later time is also close to the ground state ϕ in H^1 norm.

Theorem 3 (Instability by blow up in 2D). *At critical dimension $d = 2$, all the H^1 solutions of time-independent GPE (2.15) are unstable for GPE in the following sense: Let $\phi \in H^1(\mathbb{R}^d)$ be the ground state solution of (2.15). For any $\epsilon > 0$, there exists a function $\varphi \in H^1$, with $|\varphi - \phi|_{L^2} < \epsilon$, such that the solution ψ of (2.16) with initial condition φ , satisfies $\lim_{t \rightarrow T} |\nabla \psi|_{L^2} = \infty$, for some $0 < T < \infty$.*

This theorem tells that there exist a perturbation of ground state ϕ in 2D that makes the solution blows up in a finite time. We can use the fact that the energy of a stationary soliton in 2D is zero and the variance identity to prove it. Let $\varphi = (1 + \epsilon)\phi$, then we get the energy of φ is negative, and hence the solution satisfies $\psi(x, 0) = \varphi$ blows up.

In fact, in 2D there exist explicit solutions whose mass are equal to the mass of solitons that blow up in a finite time [11]. They have the form

$$\psi(x, t) = \frac{1}{t^* - t} \phi\left(\frac{x}{t^* - t}\right) e^{\frac{i}{t^* - t} \left(-\frac{|x|^2}{2} + 1\right)},$$



where t^* is the time at which solutions blow up. For solutions which blow up in a finite time and their mass greater than the mass of solitons, they have the asymptotic form [7] [10] [11]

$$\psi(x, t) \approx \frac{1}{L(t)} P\left(\frac{|x|}{L(t)}, b(t)\right) e^{i(\tau(t) - a(t) \frac{|x|^2}{2L^2(t)})}$$

near the singularity. The scaling factor $L(t)$ has the asymptotic form

$$L(t) \approx \left(\frac{2\pi(t^* - t)}{\ln \ln \frac{1}{t^* - t}} \right)^{\frac{1}{2}}.$$

These tell us the asymptotic behaviour of the solutions near the blow-up time.



3. Numerical methods

3.1 Gradient flow method for finding solitons in 2D

In the previous section, we see that a wave function ϕ_μ which describes the profile of a bright soliton, is a ground state of BEC with external potential $V(x) = 0$ and interaction coefficient $g < 0$. It satisfies the time-independent GPE

$$-\frac{1}{2}\Delta\phi_\mu - \mu\phi_\mu + g|\phi_\mu|^2\phi_\mu = 0,$$

and minimizes the action

$$S(\phi) = \int_{\mathbb{R}^d} \frac{1}{4}|\nabla\phi|^2 - \frac{\mu}{2}|\phi|^2 + \frac{g}{4}|\phi|^4 dx.$$

In 1D, we have the exact solution of bright solitons (the hyperbolic secant family). But in dimensions $d > 1$, we have to solve the equation numerically to find the solutions of bright solitons.

The gradient flow with discrete normalization

We use the gradient flow with discrete normalization (GFDN) method to compute the ground states, and use backward Euler sine pseudospectral (BESP) method to discretize it. This numerical method is from [2].

When we use GFDN method, we are not specifying the value of μ and then compute the corresponding ϕ_μ . We compute the ground state under certain normalization and compute the corresponding chemical potential μ .

Choose a time step $\tau = \Delta t$ and set $t_n = n\Delta t$ for $n = 0, 1, \dots$. The gradient flow with discrete normalization is as follows

$$\frac{\partial}{\partial t} \phi(x, t) = -\frac{\delta S(\phi)}{\delta \phi} = \left(\frac{1}{2} \nabla^2 + \mu - g|\phi|^2 \right) \phi(x, t), \quad x \in \mathbb{R}^d, t > 0, \quad (3.1)$$

$$\phi(x, t_{n+1}) = \frac{\phi(x, t_{n+1}^-)}{\|\phi(\cdot, t_{n+1}^-)\|}, \quad x \in \mathbb{R}^d, n \geq 0, \quad (3.2)$$

$$\phi(x, 0) = \psi_0(x), \quad x \in \mathbb{R}^d \quad \text{with } \|\psi_0\| = 1. \quad (3.3)$$

Since the wave functions we are interested in tends to zero exponentially as $|x| \rightarrow \infty$, we can approximate the function in a bounded domain and choose the homogeneous Dirichlet boundary condition. Following we set $x \in \Omega$, where Ω is a bounded domain.

For discretizing the gradient flow, we use backward Euler method for temporal discretization and sine pseudospectral method for spatial derivatives (BESP).

We present the numerical method in 1D. Choosing $\Omega = (a, b)$ and mesh size $h = \Delta x > 0$ with $h = (b - a)/M$ for M an even positive integer. Set the grid points $x_j = a + j\Delta x$, $j = 0, 1, \dots, M$. Then the scheme is

$$\frac{\phi_j^* - \phi_j^n}{\tau} = \frac{1}{2} D_{xx}^s \phi_j^* |_{x=x_j} + \mu_{\phi^n} \phi_j^* - g|\phi_j^n|^2 \phi_j^*, \quad j = 1, 2, \dots, M-1, \quad (3.4)$$

$$\phi_0^* = \phi_M^* = 0, \quad \phi_j^0 = \phi_0(x_j), \quad j = 0, 1, \dots, M, \quad (3.5)$$

$$\phi_j^{n+1} = \frac{\phi_j^*}{\|\phi^*\|}, \quad j = 0, 1, \dots, M, \quad n = 0, 1, \dots, \quad (3.6)$$

where μ_{ϕ^n} is the approximation of chemical potential of ϕ^n and D_{xx}^s is a spectral differential operator approximation of ∂_{xx} . The chemical potential of a wave function ϕ which satisfies the time-independent GPE can be computed as

$$\mu_\phi = \frac{\int \frac{1}{2} |\nabla \phi|^2 + g|\phi|^4 dx}{\int |\phi|^2 dx} = \frac{\frac{1}{2} \|\nabla \phi\|_2^2 + g\|\phi^2\|_2^2}{\|\phi\|_2^2}.$$

We use discrete sine transform method to approximate the gradient of ϕ^n , and the 2-norm is designed as $\|\phi^n\|_2^2 = h \sum_{j=1}^{M-1} |\phi_j^n|^2$ (1D). Thus μ_{ϕ^n} can be computed.



The spectral differential operator D_{xx}^s is defined as

$$D_{xx}^s \phi|_{x=x_j} = -\frac{2}{M} \sum_{l=1}^{M-1} \mu_l^2 (\hat{\phi})_l \sin(\mu_l(x_j - a)), \quad j = 1, 2, \dots, M-1.$$

where $\mu_l = \frac{\pi l}{b-a}$ and $(\hat{\phi})_l$ ($j = 1, 2, \dots, M-1$) are the discrete sine transform coefficients of ϕ_j ($j = 1, 2, \dots, M-1$). We solve the equation (3.4) by introducing a stabilization term with constant coefficient α

$$\frac{\phi_j^{*,m+1} - \phi_j^n}{\tau} = \frac{1}{2} D_{xx}^s \phi^{*,m+1}|_{x=x_j} - \alpha \phi_j^{*,m+1} + (\alpha + \mu_{\phi^n} - g|\phi_j^n|^2) \phi_j^{*,m},$$

$$m = 0, 1, 2, \dots, \quad (3.7)$$

$$\phi_j^{*,0} = \phi_j^n, \quad j = 0, 1, \dots, M. \quad (3.8)$$

The α is called the optimal stabilization parameter suggested as [2]

$$\alpha = \frac{1}{2}(b_{\max} + b_{\min}),$$

where

$$b_{\max} = \max_{1 \leq j \leq M-1} (-\mu_{\phi^n} + g|\phi_j^n|^2),$$

$$b_{\min} = \min_{1 \leq j \leq M-1} (-\mu_{\phi^n} + g|\phi_j^n|^2).$$

To solve (3.7), we take discrete sine transform at both sides of it and obtain

$$\frac{(\widehat{\phi_j^{*,m+1}})_l - (\widehat{\phi_j^n})_l}{\tau} = -\left(\alpha + \frac{1}{2}\mu_l^2\right) (\widehat{\phi_j^{*,m+1}})_l + (\widehat{G_j^m})_l, \quad l = 1, 2, \dots, M-1, \quad (3.9)$$

where $(\widehat{G_j^m})_l$ are the discrete sine transform coefficients of G_j^m defined as

$$G_j^m = (\alpha + \mu_{\phi^n} - g|\phi_j^n|^2) \phi_j^{*,m}, \quad j = 1, 2, \dots, M-1.$$

We rewrite (3.9) to get

$$(\widehat{\phi^{*,m+1}})_l = \frac{2}{2 + \tau(2\alpha + \mu_l^2)} \left((\widehat{\phi^n})_l + \tau(\widehat{G^m})_l \right), \quad l = 1, 2, \dots, M-1. \quad (3.10)$$



And taking inverse discrete sine transform, then we get $\phi^{*,m+1}$.

We need to specify the type of norm in (3.6). Usually we use 2-norm for measuring wave functions, but in the 2D case, we can't use 2-norm to compute the ground state. The reason is that we can't assign the total mass and compute the corresponding wave function of soliton in 2D, since the mass of every solitons in 2D are all the same. We shall use the uniform norm $\|\psi^n\| = \max_j(\phi_j^n)$ instead. The ground state we find here is a soliton with height 1.

Tests of the gradient flow method

We define numerical residual by

$$err = \max_j \left(\frac{1}{2} D_{xx}^s \phi^n|_{x=x_j} + \mu_{\phi^n} \phi_j^n - g|\phi_j^n|^2 \phi_j^n \right).$$

The stopping criterion for the above backward iteration scheme is when the residual error reaches some prescribed value. Here, we choose it to be 1E-12. The density profile so obtained is shown in Figure 3.1.

3.2 TSSP method for computing the dynamics of BECs

We use the time-splitting sine pseudospectral (TSSP) method to solve the GPE with a given initial wave function. This algorithm was constructed by Weizhu Bao [1], it is fast and unconditionally stable.

Since the wave functions which we are concerned about tend to zero as x tends to infinity, we can solve the GPE in a bounded domain which is large enough, and set the values of the wave functions at the boundary to be zero. Hence it becomes an initial boundary value problem with homogeneous Dirichlet boundary condition. We represent the problem in

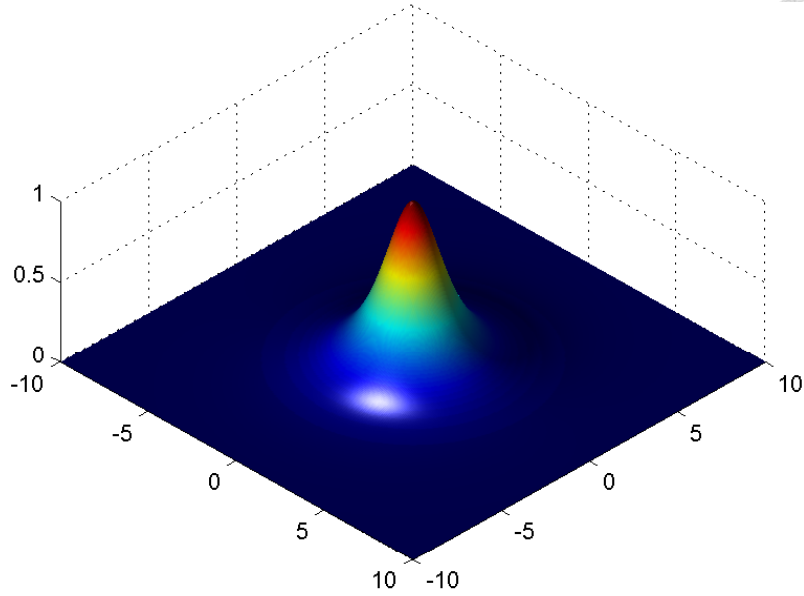


Figure 3.1: Soliton in 2D with $\|\phi\|_\infty = 1$

1D:

$$i\partial_t \psi(x, t) = -\frac{1}{2}\psi_{xx}(x, t) + V(x)\psi(x, t) + g|\psi|^2\psi(x, t), \quad x \in (a, b), t > 0,$$

$$\psi(x, 0) = \psi_0(x), \quad x \in [a, b],$$

$$\psi(a, t) = \psi(b, t) = 0, \quad t > 0.$$

Now we consider an initial value problem

$$\frac{d}{dt}u(t) = (A + B)u(t), \quad u(0) = f(x), \quad (3.11)$$

where A and B are two operators, the solution can be written in the form $u(t) = e^{t(A+B)}u(0)$.

In general, A does not commute with B , so $u(t) \neq e^{tA}e^{tB}u(0)$. But by using Taylor expansion, we have

$$u(t + \Delta t) = e^{\Delta t A}e^{\Delta t B}u(t) + O(\Delta t).$$

This implies that if Δt is small, then we can approximate $u(t + \Delta t)$ by $e^{\Delta t A}e^{\Delta t B}u(t)$, and hence we can solve the two operators A and B separately. This is an example of time-splitting approximation. Let $\Delta t = \tau > 0$, $t_n = n\tau$, and u^n be the numerical approx-

imation of $u(t_n)$. There are two splitting methods commonly used to solve (3.11)

$$u^{n+1} = e^{\tau A} e^{\tau B} u^n, \quad \text{Lie-Trotter splitting,}$$

$$u^{n+1} = e^{\tau A/2} e^{\tau B} e^{\tau A/2} u^n, \quad \text{Strang splitting.}$$



The error of Lie-Trotter splitting is of first order $O(\tau)$, and the error of Strang splitting is of second order $O(\tau^2)$.

In our case GPE, we choose

$$A\psi = \frac{i}{2} \partial_{xx} \psi, \quad B\psi = -i(V + g|\psi|^2)\psi,$$

and use the Strang splitting. From t_n to t_{n+1} , we solve $\psi^{(1)} = e^{\tau A/2} \psi$, $\psi^{(2)} = e^{\tau B} \psi^{(2)}$, and $\psi^{n+1} = e^{\tau A/2} \psi^{(2)}$ to get ψ^{n+1} from ψ^n . To solve $\psi^{(1)} = e^{\tau A/2} \psi^n$, we first write

$$\psi^n = \sum_l (\widehat{\psi^n})_l \sin(\mu_l(x - a)),$$

where $\mu_l = l\pi/(b - a)$, $l = 1, \dots, M - 1$, $(\widehat{\psi^n})_l$ are the discrete sine transform coefficients of ψ^n . Hence

$$A\psi^n = \frac{i}{2} \partial_{xx} \psi^n = \frac{i}{2} \sum_l (-\mu_l^2) (\widehat{\psi^n})_l \sin(\mu_l(x - a)),$$

the second derivative of ψ^n is obtained by multiplying it's Fourier coefficients by $-\mu_l^2$, and thus we get

$$\psi^{(1)} = e^{\tau A/2} \psi^n = \sum_l e^{\frac{i}{2}(-\mu_l^2)\tau/2} (\widehat{\psi^n})_l \sin(\mu_l(x - a)).$$

For solving $\frac{\partial}{\partial t} \psi = B\psi$, since $|\psi|$ is invariant in t in this ODE, it can be integrate exactly, we get

$$\psi^{(2)} = e^{\tau B} \psi^{(1)} = e^{-i(V + g|\psi^{(1)}|^2)\tau} \psi^{(1)}.$$



Let mesh size $\Delta x = h$, $x_j = jh + a$, $j = 0, \dots, M$, $M = (b - a)/h$, and ψ_j be the numerical approximation of $\psi(x_j, t)$. The complete algorithm is

$$\begin{aligned}\psi_j^{(1)} &= \frac{2}{M} \sum_{l=1}^{M-1} e^{-i\tau\mu_l^2/4} (\widehat{\psi^n})_l \sin(\mu_l(x_j - a)), \\ \psi_j^{(2)} &= e^{-i(V(x_j) + \beta|\psi_j^{(1)}|^2)\tau} \psi_j^{(1)}, \quad j = 1, \dots, M-1 \\ \psi_j^{n+1} &= \frac{2}{M} \sum_{l=1}^{M-1} e^{-i\tau\mu_l^2/4} (\widehat{\psi^{(2)}})_l \sin(\mu_l(x_j - a)), \quad \psi_0^{n+1} = \psi_M^{n+1} = 0\end{aligned}$$

where $\mu_l = l\pi/(b - a)$, and $(\widehat{\psi^n})_l$ and $(\widehat{\psi^{(2)}})_l$ are the discrete sine transform coefficients of ψ^n and $\psi^{(2)}$, respectively.

TSSP method is faster than finite difference method, since it uses fast Fourier transform to solve the differential equation. And since the integrations are all exact, it is unconditionally stable.

Tests of TSSP method

We use the bright soliton solutions to test the TSSP method.

- **Case 1: 1D soliton**

First we test the method in 1D. The 1D soliton solutions are

$$\psi(x, t) = \eta \operatorname{sech}(\eta(x - vt)) e^{i(kx - \omega t)},$$

where $v \equiv \partial\omega/\partial k = k$, $\omega = \frac{1}{2}(k^2 - \eta^2)$. We choose $\eta = 1$, $k = 2$, and hence $\omega = 1.5$ and $v = 2$. The bright soliton becomes

$$\psi(x, t) = \operatorname{sech}(x - 2t) e^{i(2x - \frac{3}{2}t)},$$

the initial condition is taken as

$$\psi(x, 0) = \operatorname{sech}(x) e^{i2x},$$

h	1/2	1/4	1/8	1/16
error	4.580E-3	8.595E-7	8.622E-7	8.622E-7



Table 3.1: Errors for $\tau = 1/1024$ and various values of h (case 1)

τ	1/8	1/16	1/32	1/64
error	1.397E-2	3.521E-3	8.821E-4	2.206E-4
τ	1/128	1/256	1/512	1/1024
error	5.517E-5	1.379E-5	3.448E-6	8.622E-7

Table 3.2: Errors for $h = 1/16$ and various values of τ (case 1)

we solve this on $[-64, 64]$, and check the results at $t = 10$, the mesh size and time step are h and τ , respectively.

Table 3.1 lists the errors in sup norm for $\tau = 1/1024$ and various spatial mesh sizes h . We see that the error decreases very fast when h is reduced from 1/2 to 1/4, then saturated. This means that the temporal error dominates. Table 3.2 lists the errors in sup norm for $h = 1/16$ and various time steps τ . From these two tests, we see that the method is spectrally accurate in space and second order accurate in time.

• Case 2: 2D soliton

In general, the soliton solution is

$$\psi(x, t) = \phi(x - vt) e^{i(v \cdot x - \frac{|v|^2}{2}t + \omega t)},$$

where ϕ is real and satisfies the equation

$$-\frac{1}{2}\Delta\phi(x) + \omega\phi(x) - \phi^3(x) = 0.$$

We use BESP method to find the 2D soliton centered at the origin $(0, 0)$ with height 1 ($\max(\phi) = 1$), and denote the wave function by ϕ_1 . The value of ω for ϕ_1 can be computed numerically, so we know the solution at any time with a given velocity v .

τ	1/8	1/16	1/32	1/64
error	1.210E-2	3.084E-3	7.747E-4	1.939E-4
τ	1/128	1/256	1/512	1/1024
error	4.850E-5	1.213E-5	3.031E-6	7.579E-7



Table 3.3: Errors for $h = 1/16$ and various values of τ (case 2)

We take the initial wave function as

$$\psi(x, 0) = \phi_1(x) e^{i(v \cdot x)},$$

with $v = (2, 1)$, solve the GPE on $(-32, 32) \times (-32, 32)$, and check the results at $t = 5$. Table 3.3 lists the errors in sup norm for $h = 1/16$ and various time steps τ . We see that the error is also of $O(\tau^2)$.

• **Case 3: Two solitons in 2D**

In this case we test TSSP method by using it to solve coupled GPEs:

$$\begin{aligned} i \frac{\partial}{\partial t} \psi_1 &= -\frac{1}{2} \nabla^2 \psi_1 + (g_{11} |\psi_1|^2 + g_{12} |\psi_2|^2) \psi_1, \\ i \frac{\partial}{\partial t} \psi_2 &= -\frac{1}{2} \nabla^2 \psi_2 + (g_{21} |\psi_1|^2 + g_{22} |\psi_2|^2) \psi_2. \end{aligned}$$

If we assume that ψ_1 and ψ_2 are solitons and $\psi_2 = a\psi_1$, choose $g_{11} = g_{11} = -1$ then there are simple solutions in the form:

$$\begin{aligned} \psi_1 &= \frac{1}{\sqrt{1 - a^2 g_{12}}} \phi_\mu(x - vt) e^{i(v \cdot x - \frac{|v|^2}{2} t - \mu t)}, \\ \psi_2 &= \frac{1}{\sqrt{1 - g_{12}/a^2}} \phi_\mu(x - vt) e^{i(v \cdot x - \frac{|v|^2}{2} t - \mu t)}, \end{aligned}$$

τ	1/8	1/16	1/32	1/64
error(ψ_1)	5.410E-3	1.379E-3	3.465E-4	8.673E-5
error(ψ_2)	1.082E-2	2.758E-3	6.930E-4	1.735E-4
τ	1/128	1/256	1/512	1/1024
error(ψ_1)	2.169E-5	5.423E-6	1.356E-6	3.389E-7
error(ψ_2)	4.338E-5	1.085E-5	2.711E-6	6.779E-7



Table 3.4: Errors for $h = 1/16$ and various values of τ (case 3)

where ϕ_μ is the same as in section 2, a and g_{12} satisfy the following equations

$$(g_{12} + 1)(a^2 - 1) = 0,$$

$$g_{12} - a^2 < 0,$$

$$g_{12}a^2 - 1 < 0.$$

We choose $a = 2$, $g_{12} = -1$, $v = (2, 1)$, ϕ_μ same as in case 2 (with height 1), solve the coupled GPEs in $(-32, 32) \times (-32, 32)$, and check the results at $t = 5$.

Table 3.4 lists the errors in sup norm for $h = 1/16$ and various time steps τ .



4. Numerical examples

4.1 Examples of one-component BEC: perturbations of solitons

In this subsection, we perturb the amplitude of a static soliton and solve the evolution of the wave packet. We can see the stability/instability of solitons under this kind of perturbations.

The initial value problem is

$$\begin{aligned}i\partial_t\psi(x, t) &= -\frac{1}{2}\psi_{xx}(x, t) - |\psi|^2\psi(x, t), \quad x \in \Omega, t > 0, \\ \psi(x, 0) &= \psi_0(x), \quad x \in \Omega, \\ \psi(x, t)|_{x \in \Omega} &= 0, \quad t > 0.\end{aligned}$$

The initial condition is taken as

$$\psi_0(x) = (1 \pm \epsilon)\phi(x),$$

where ϕ is the ground state which satisfies the time-independent GPE (2.15) with $g = -1$.

We solve this problem by the TSSP method presented in section 4.



Example 1: Perturbations of a soliton in 1D

In example 1 we solve the above problem in 1D. We specify the initial condition as

$$\psi(x, 0) = (1 + \epsilon)\phi(x),$$

where $\phi(x) = \text{sech}(x)$ is the shape function of a soliton in 1D.

We solve this initial value problem on $\Omega = (-16, 16)$ and choose the mesh size $h = 1/16$ and time step $\tau = 1/1024$.

Figure 4.1 shows the density profile $|\psi(x)|^2$ of the wave packet at different times, with $\epsilon = 0.01$. We see that the shape of the wave packet does not change very much in time.

Next we observe the difference between this wave function and the original soliton. For

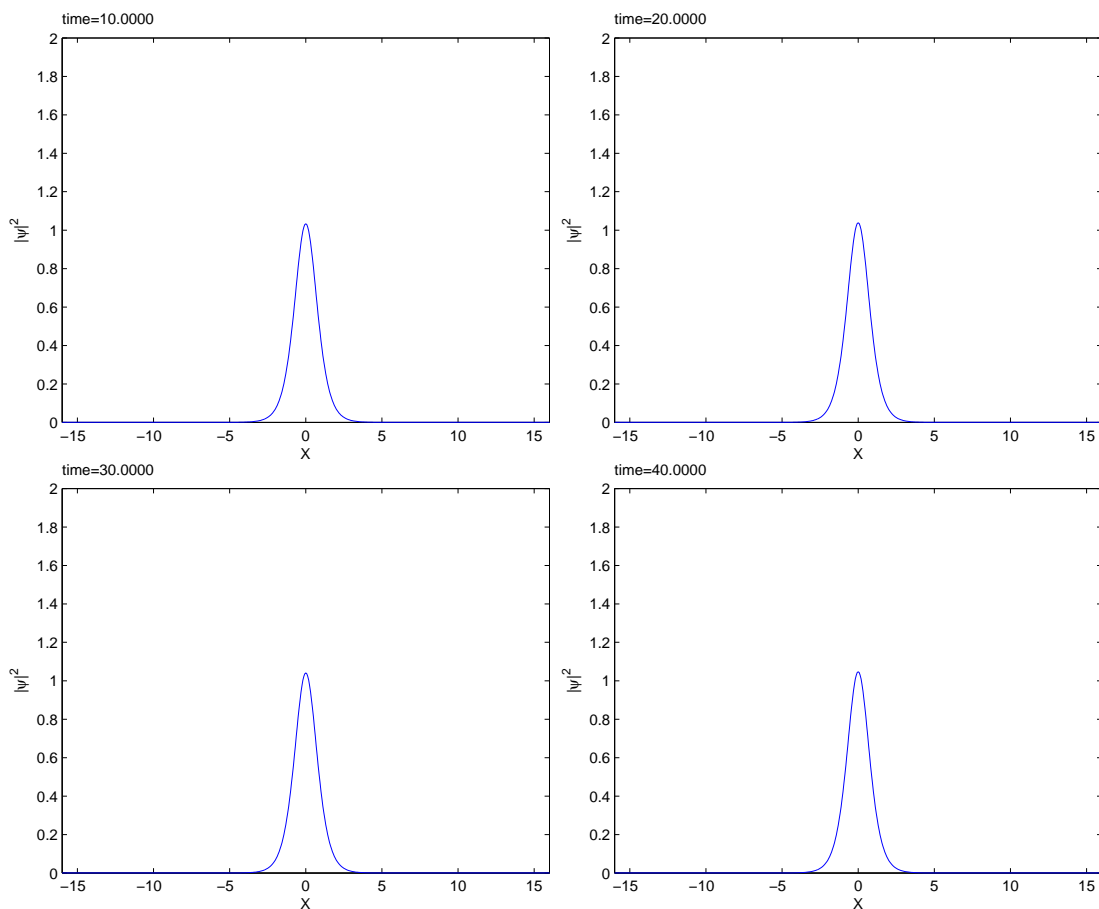


Figure 4.1: Density profile of $|\psi|^2$ at different time for $\epsilon = 0.01$

convenience, we only measure the difference between the absolute values of them. The

difference is defined as

$$d(\psi, \phi) = \|\psi(\cdot, t) - \phi(\cdot)\|_{H^1}.$$

The difference vs. time graph is shown in Figure 4.2. We see that the it is bounded in time.

Figure 4.3 shows the difference vs. time graph with $\epsilon = 0.001$ and $\epsilon = 0.0001$. Obviously

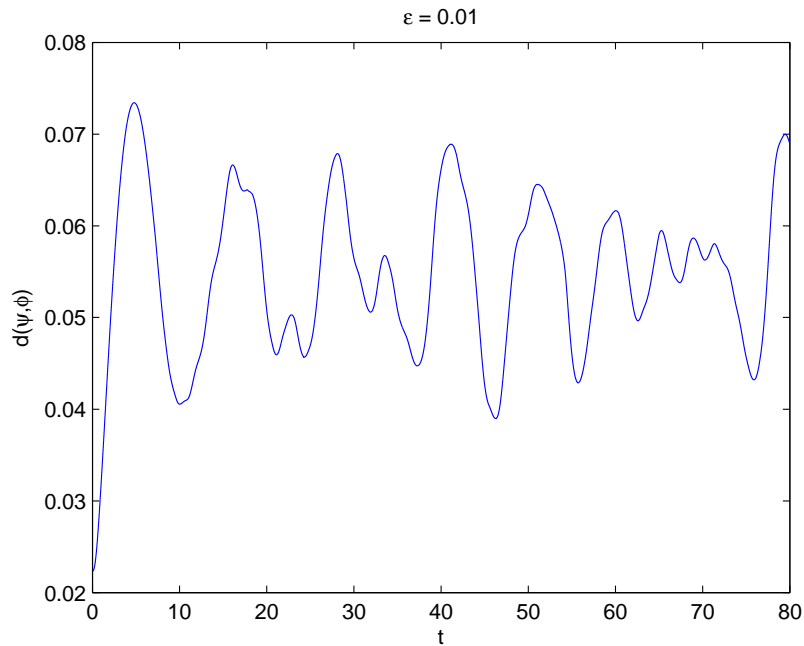


Figure 4.2: Difference vs. time graph for $\epsilon = 0.01$

the difference is less as ϵ is less. This result is consistent with the fact that soliton in 1D is (orbitally) stable.

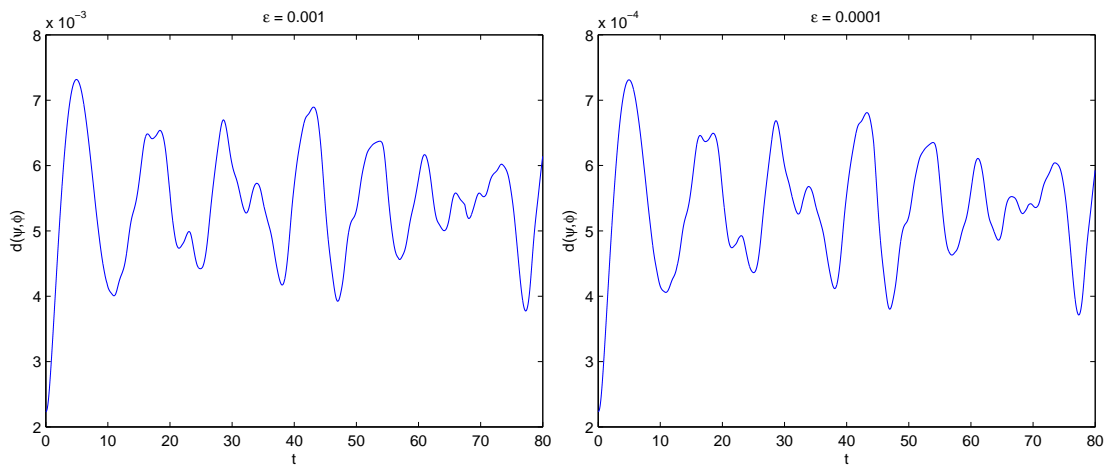
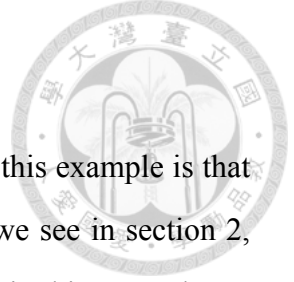


Figure 4.3: Difference vs. time graph for $\epsilon = 0.001, 0.0001$



Example 2: Perturbations of a soliton in 2D

In example 2 we solve the same problem in 2D. The crucial point in this example is that the mass of the wave packets are changed by the perturbation. As we see in section 2, the mass of all solitons in 2D are all the same. Thus the wave packets in this example are no longer solitons and their behaviour will be different. We split this example into two cases, one for a smaller amplitude of perturbation, and the other for a greater amplitude of perturbation.

Case 1: Smaller mass than that of a soliton We take the initial condition as

$$\psi(x, 0) = 0.99 \phi(x),$$

where ϕ is the ground state satisfies the time-independent GPE (2.15) in 2D, with $g = -1$. It also satisfies

$$\begin{aligned}\phi(x) &> 0 \\ \|\phi(x)\|_{\infty} &= \phi(0, 0) = 1.\end{aligned}$$

We solve this initial value problem on $\Omega = (64, 64)^2$ and choose the mesh size $h = 1/16$ and time step $\tau = 1/1024$.

Figure 4.4 shows the density profile $|\psi|^2$ of the wave packet at different times, we see that it spreads out in time.

We check the results by the variance identity. As discussed in section 2, the energy of a static soliton is zero. The kinetic energy and interaction energy of a static soliton in 2D have the same magnitude but are opposite in sign. Let C be the kinetic energy of ϕ , then we have

$$\begin{aligned}E(\psi) &= [(1 - \epsilon)^2 - (1 - \epsilon)^4] \cdot C \\ &\approx [(1 - 2\epsilon) - (1 - 4\epsilon)] \cdot C = 2\epsilon \cdot C > 0.\end{aligned}$$

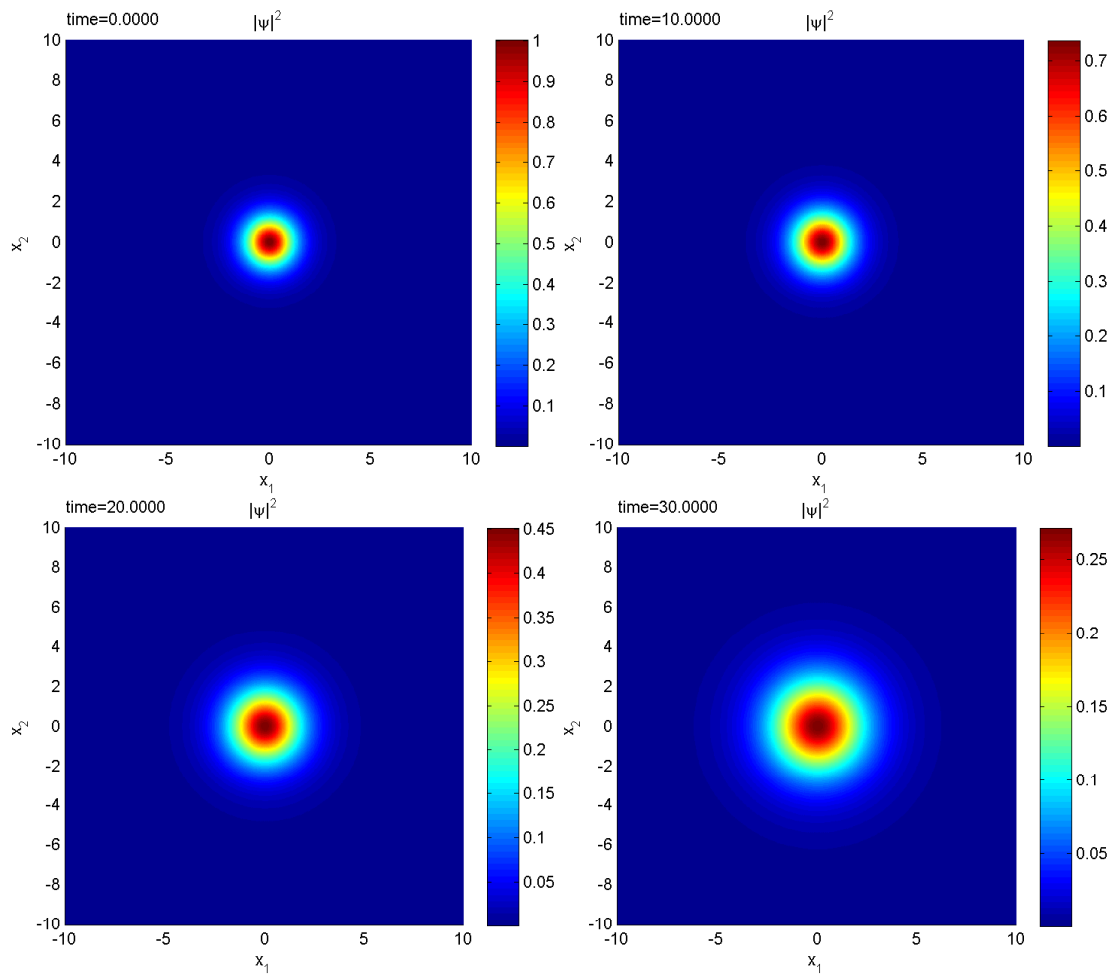


Figure 4.4: $|\psi(x)|^2$ at different time (case 1)

Hence by the variance identity, the wave packet should eventually spread out (blow up cannot happen since its total mass is less than the mass of a soliton).

Figure 4.5 shows the energy vs. time graph and Figure 4.6 shows the width w

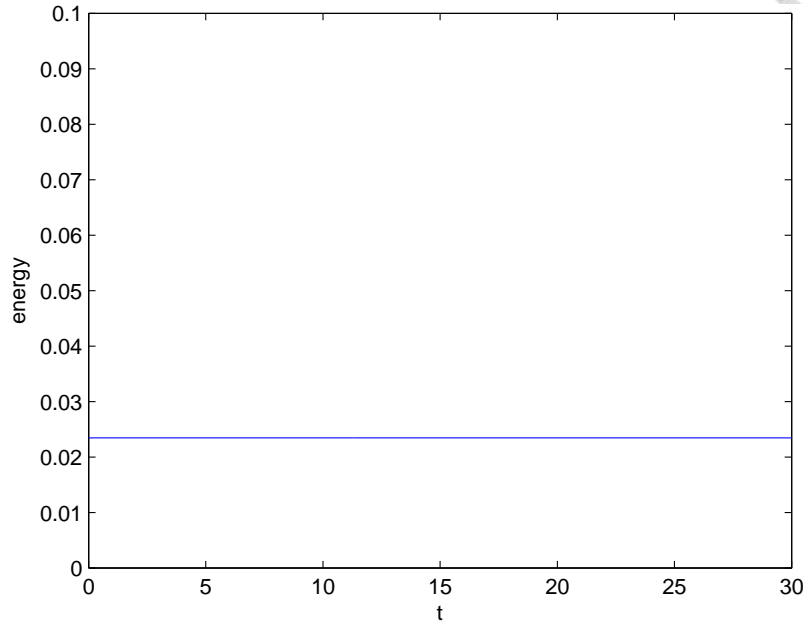


Figure 4.5: Energy vs. time graph (case 1)

(in this case it equals the variance since $\langle x \rangle = (0, 0)$) vs. time graph. We see that the energy is both constant and positive. The curve on the w vs. time graph fits a quadratic curve very well, as suggested by the variance identity in 2D. The difference between the quadratic coefficient of the curve and two times of the energy is $2.996E-5$.

This result matches our expectation, since a wave packet can not keep its shape unchanged or even blow up with its mass less than the mass of a soliton.

Case 2: Greater mass than that of a soliton In this case we take the initial condition as

$$\psi(x, 0) = 1.01\phi(x),$$

where $\phi(x)$ is same as in case 1.

We solve this initial value problem on $(32, 32)^2$ and choose the mesh size $h = 1/32$, time step $\tau = 1/1024$.

Figure 4.7 shows the density profile $|\psi(x)|^2$ at different times, and Figure 4.8 shows

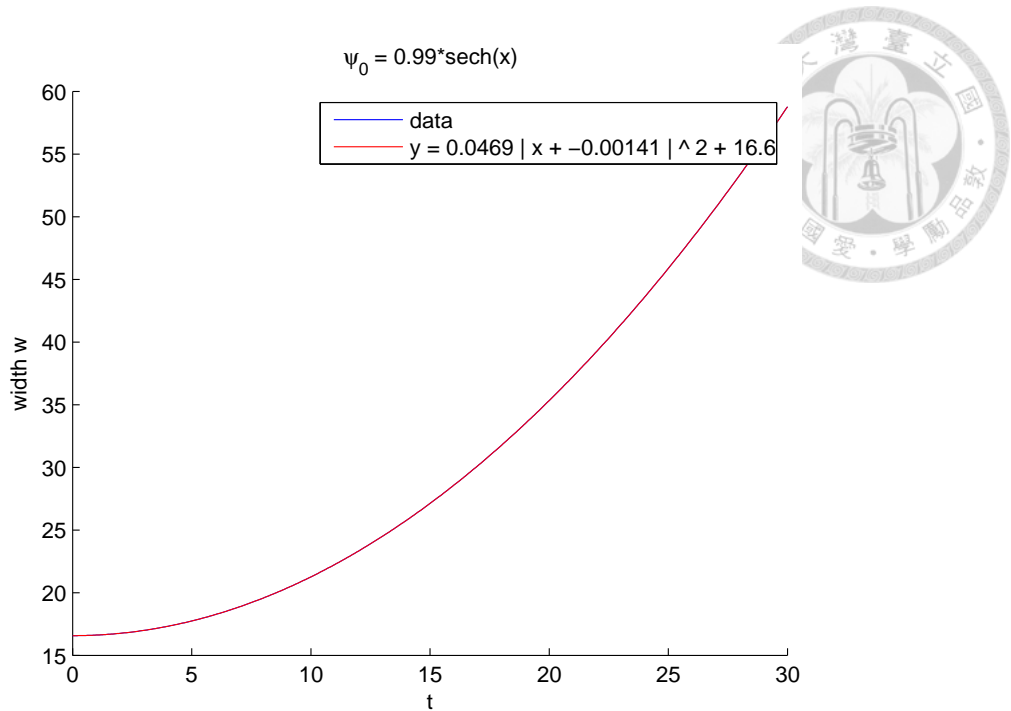


Figure 4.6: w vs. time graph (case 1)

the maximum of $|\psi(x)|^2$ vs. time graph. We see that the solution grows up quickly near the time $t = 18.578$.

To check whether it blows up at that time, we observe the energy E and the width w of the solution vs. time graph shown in Figure 4.9 and Figure 4.10, respectively. In Figure 4.9, we find that the energy is not conserved at that time. This tells us that the solution exceeds the limitation of the computing. On the other hand, the energy before $t = 18.578$ is negative (as suggested by a similar estimate as in case 1), and hence by the variance identity the solution should blow up in a finite time.

In Figure 4.10, we see that the curve on the w vs. time graph also fits a quadratic curve very well. The difference between the quadratic coefficient of the fitting curve and two times of the energy is $2.816E-5$. The fitting curve predicts that the solution blows up at $t \approx 18.699$.

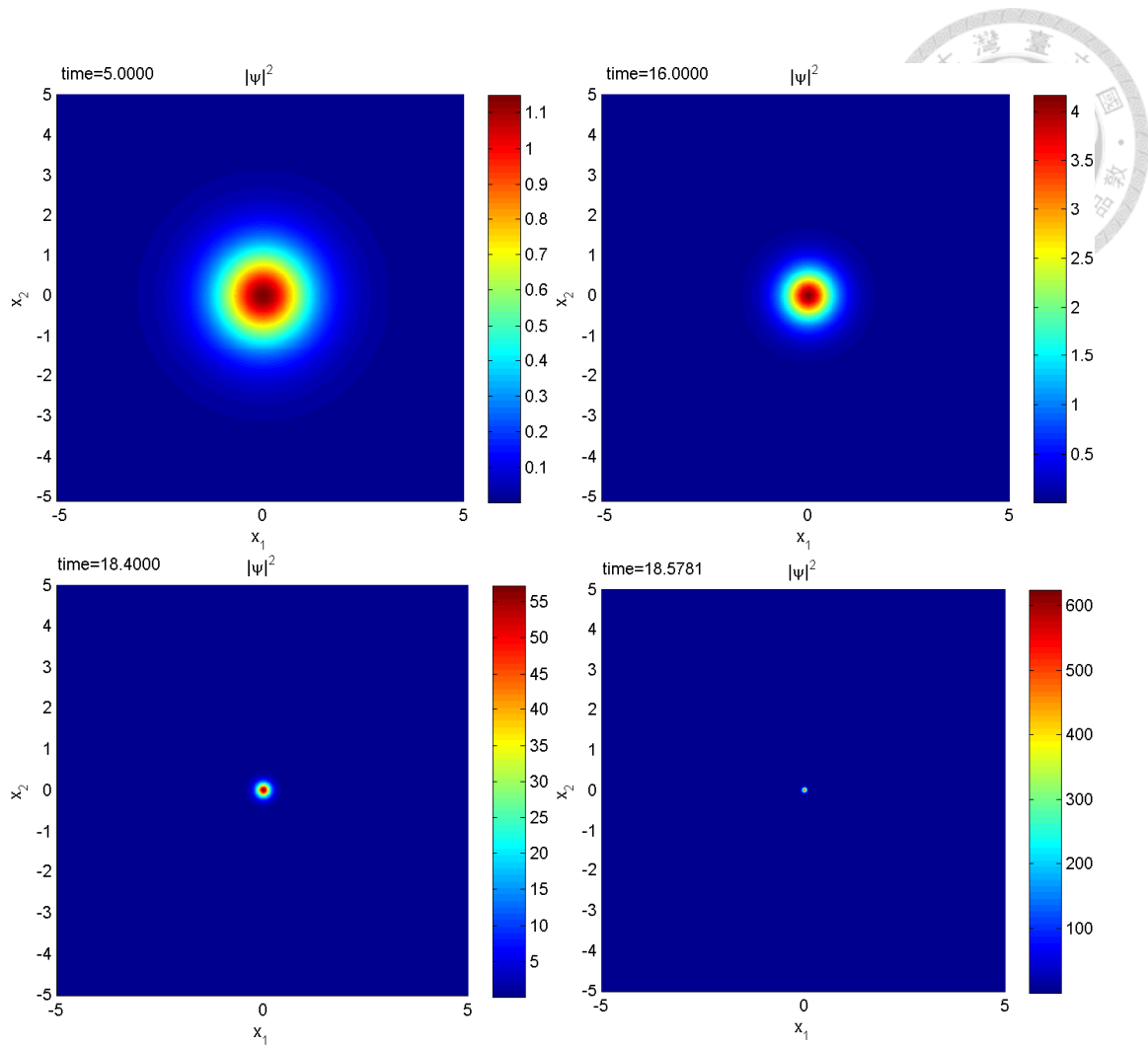


Figure 4.7: Density profile of the wave packet at different time (case 2)

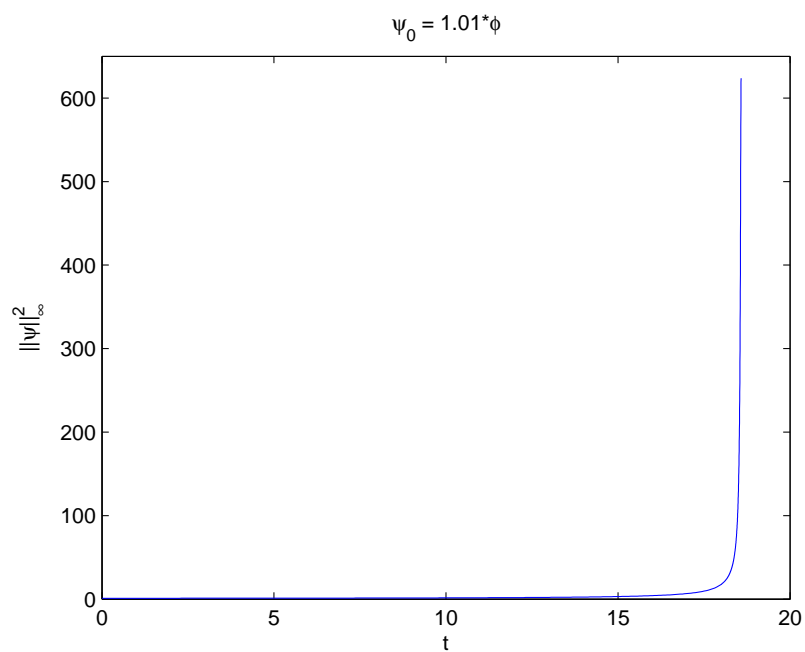


Figure 4.8: $\|\psi\|_{\infty}^2$ vs. time graph (case 2)

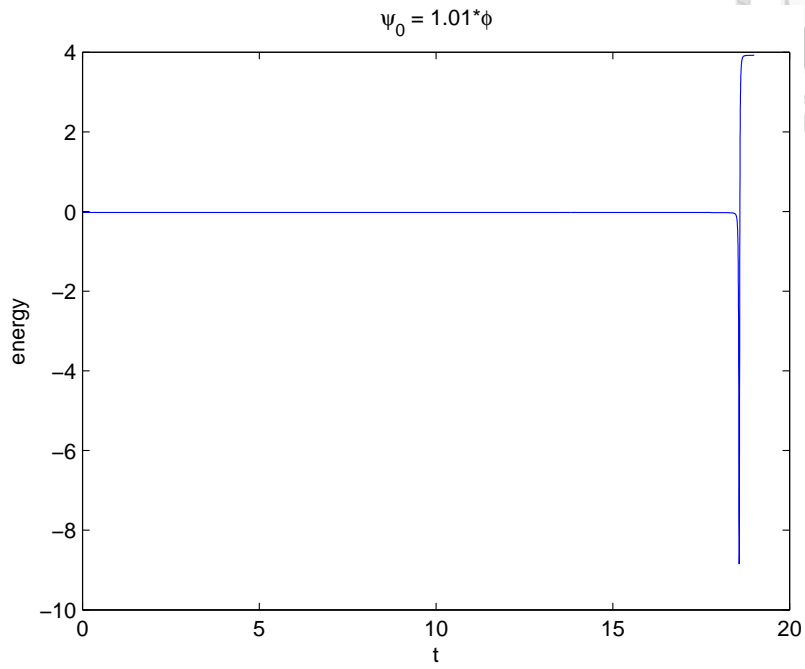
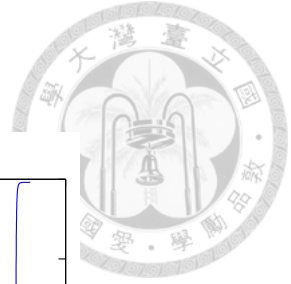


Figure 4.9: Energy vs. time graph (case 2)

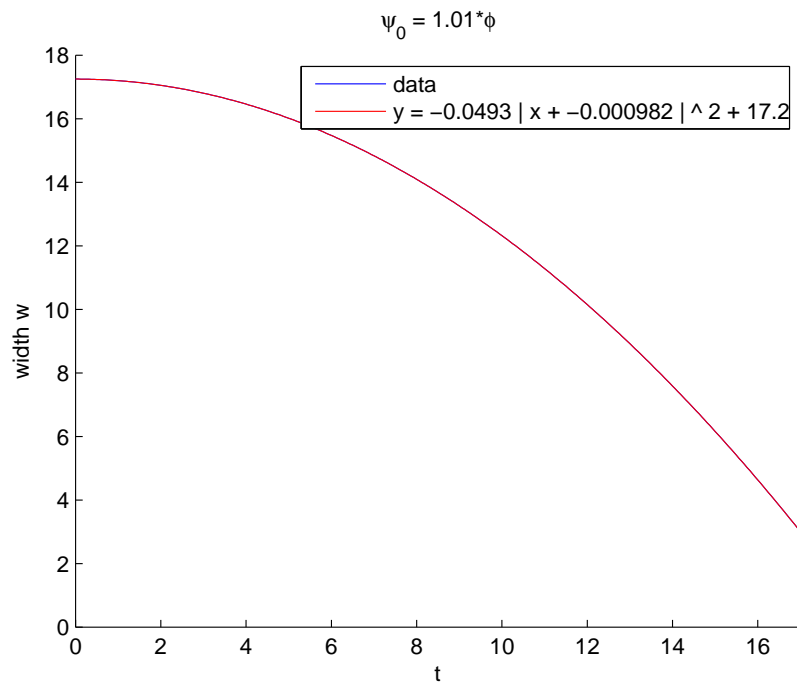


Figure 4.10: w vs. time graph (case 2)



4.2 Examples of two-component BECs: collisions of solitons

In this subsection we solve the evolutions of colliding solitons in 1D and 2D. The initial value problem is

$$\begin{aligned}
 i\frac{\partial}{\partial t}\psi_1 &= -\frac{1}{2}\Delta\psi_1 + (-|\psi_1|^2 + g_{12}|\psi_2|^2)\psi_1 & x \in \mathbb{R}^d, t > 0 \\
 i\frac{\partial}{\partial t}\psi_2 &= -\frac{1}{2}\Delta\psi_2 + (g_{21}|\psi_1|^2 - |\psi_2|^2)\psi_2 & x \in \mathbb{R}^d, t > 0 \\
 \psi_1(x, 0) &= \psi_{10}(x) & x \in \mathbb{R}^d, \\
 \psi_2(x, 0) &= \psi_{20}(x) & x \in \mathbb{R}^d,
 \end{aligned}$$

where g_{12}, g_{21} are interaction coefficients have the same value. They represent the interaction strength between the two waves (negative for attractive and positive for repulsive).

The initial conditions are of the form

$$\begin{aligned}
 \psi_{10}(x) &= \phi(x - x_{10})e^{i(v_{10} \cdot (x - x_{10}))}, \\
 \psi_{20}(x) &= \phi(x - x_{20})e^{i(v_{20} \cdot (x - x_{20}))},
 \end{aligned}$$

where $\phi(x)$ is the shape function of a soliton, x_{10}, x_{20} and v_{10}, v_{20} are center of mass and center of velocities of the two soliton at $t = 0$, respectively. The shape function ϕ of solitons is the same as the previous examples. It satisfies the time-independent GPE (2.15) with $g = -1$ and

$$\begin{aligned}
 \phi(x) &> 0, \quad x \in \mathbb{R}^d, \\
 \|\phi(x)\|_\infty &= \phi(O) = 1,
 \end{aligned}$$

where O is the origin of the space.



Example 3: Collision of two solitons in 1D

In example 3 we solve this problem in 1D. The initial conditions are taken as

$$\begin{aligned}\psi_{10}(x) &= \operatorname{sech}(x + 50) e^{i(4(x+50))}, \\ \psi_{20}(x) &= \operatorname{sech}(x + 30) e^{i(2(x+30))}.\end{aligned}$$

The initial conditions are shown in Figure 4.11. We solve this initial value problem with

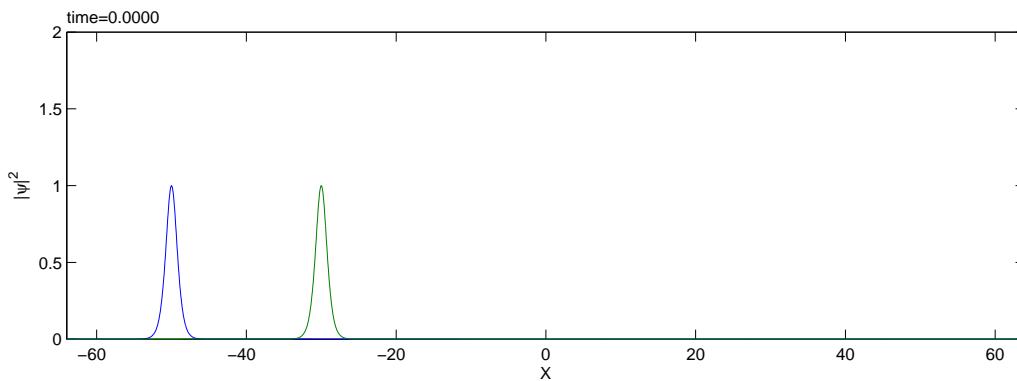


Figure 4.11: Initial conditions in example 3

different values of $g_{12} = g_{21}$, on the domain $\Omega = (-64, 64)$ and choose the mesh size $h = 1/16$ and time step $\tau = 1/1024$.

The initial center of soliton 1 and 2 are at $x = -50$ and $x = -30$, and the initial velocities are 4 and 2, respectively. At the beginning, $\psi_1\psi_2 \approx 0$, the interaction between soliton 1 and 2 are weak. After a short time, soliton 1 catches up soliton 2 and they begin to interact with each other. We discuss the dynamics during their collision with different values of interaction coefficient $g_{12} = g_{21}$.

1. Attractive $g_{12} = g_{21} \leq 0$

When $g_{12} \leq 0$, the two solitons pass through each other after collisions. If the interactions are weak ($g_{12} < 2$), then they pass through each other with both shapes almost unchanged after collisions. The density function of them at different time for $g_{12} = -2$ are shown in Figure 4.12.

When the interactions are stronger, ($g_{12} = -3, -4$), we observe that after collisions, there are small waves separate from the original solitons which will follow the other

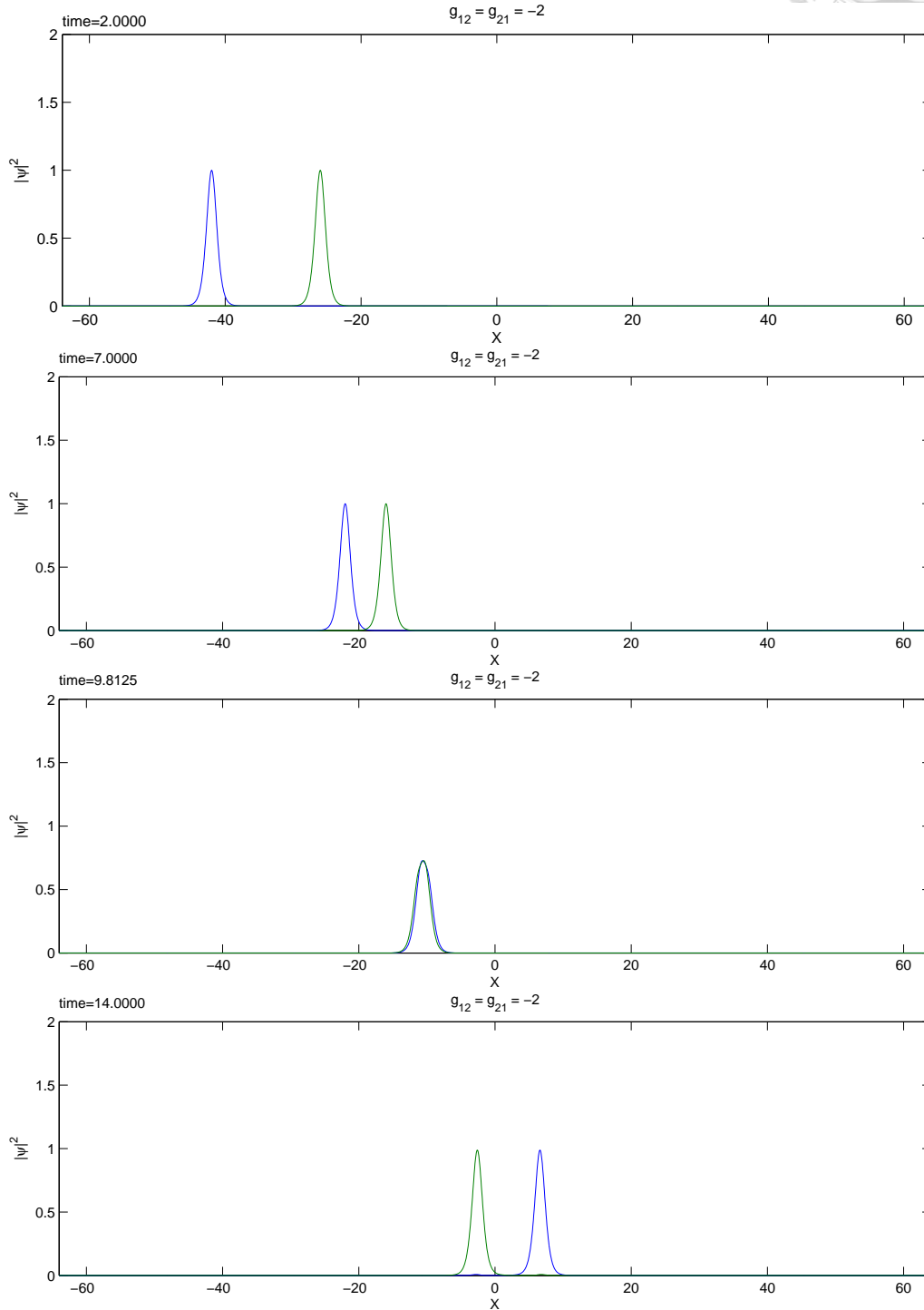
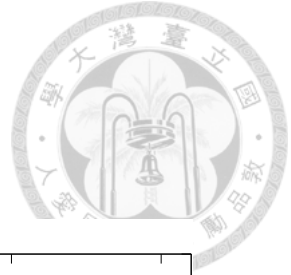


Figure 4.12: Density profiles of ψ_1 and ψ_2 at different time for $g_{12} = -2$ (example 3)

solitons, see Figure 4.13. When $g_{12} < -7$, there are second small waves in the middle of the two solitons after collision, see Figure 4.14.

Next we observe the speeds of the waves. The center of velocities change when the

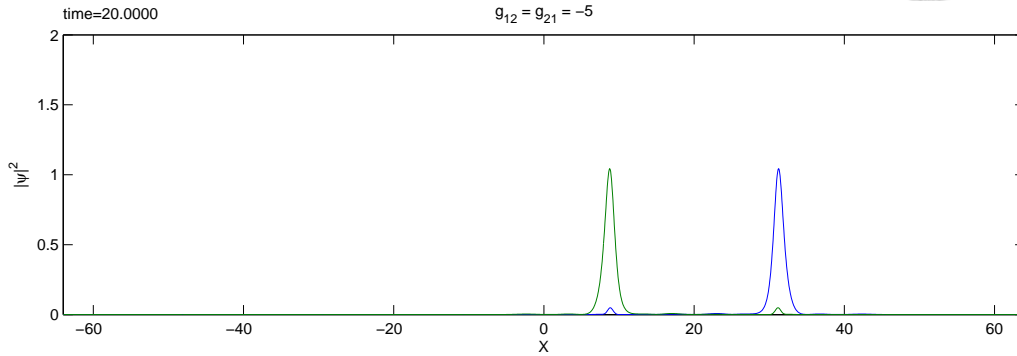


Figure 4.13: Small waves separate from original solitons ($g_{12} = -5$)

two wave packets are interacting, and hence causes position shifts after collision.

Figure 4.15 shows the velocity vs. time graph of the two solitons with different values of g_{12} .

We see that when the interactions are weak (those cases where there are no small waves separated from the original soliton after collisions), the center of velocities of them are the same before and after the collisions, but they change during the interactions. For soliton 1, we can see that it's speed increases and then decreases to the original value during the collision. While for soliton 2, the speed decreases and then increases to the original value.

This phenomenon is physically reasonable. When the two solitons are getting closer, their attractive interactions become stronger, so there is a stronger force act between

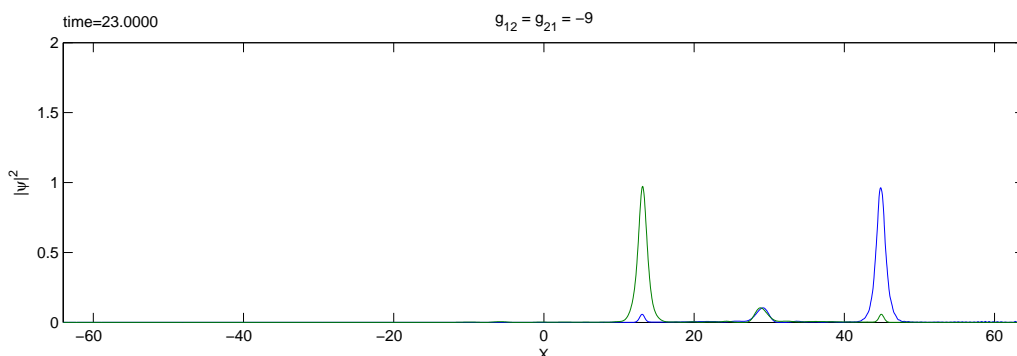


Figure 4.14: Small waves separate from original solitons ($g_{12} = -9$)

them to pull them together. We can see that the velocities change more (and thus greater position shifts) when the interaction coefficient g_{12} is lower.

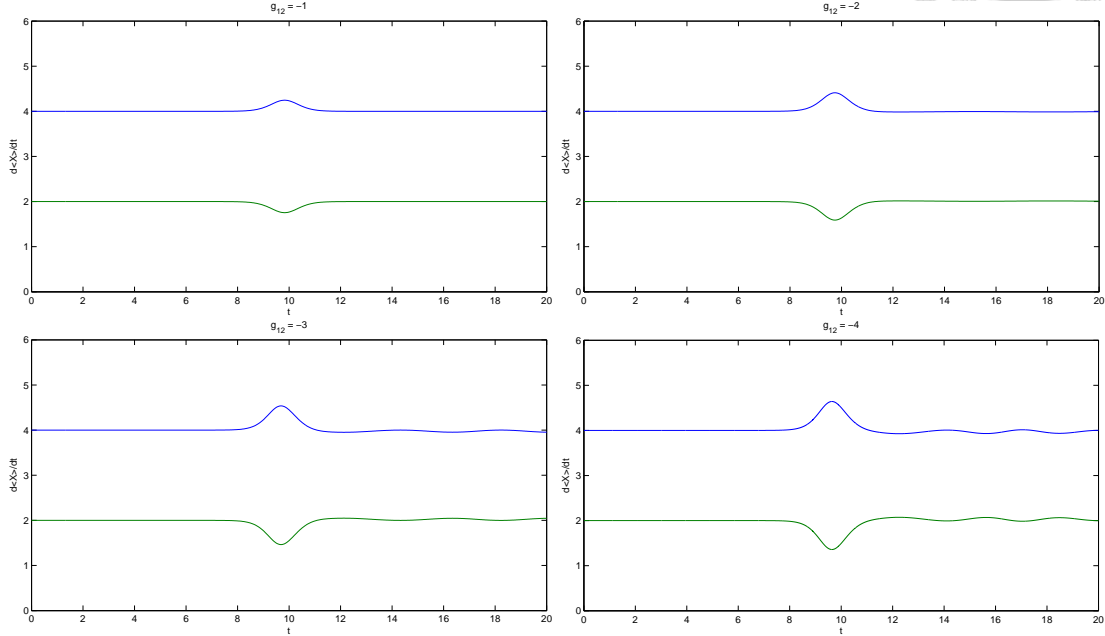
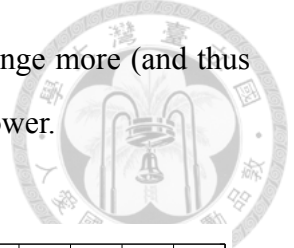


Figure 4.15: Velocity v.s. time graph of soliton 1 and 2 with different values of g_{12} (example 3)

2. Repulsive $g_{12} = g_{21} > 0$

When the interaction between solitons is repulsive, whether or not they will pass through each other depends on the strength of interactions. They can still pass through each other when the interaction is weak, and can not pass through each other when the interaction is strong enough.

Figure 4.16, Figure 4.17 and Figure 4.18 show the density functions of the two solitons at different time for interaction coefficient $g_{12} = 0.1$, $g_{12} = 1$ and $g_{12} = 5$, respectively. In the case of $g_{12} = 0.1$, we see that the solitons pass through each other and maintain their shapes during collision. In the case of $g_{12} = 0.95$, we see that parts of the solitons pass through and the other parts do not, and their shapes continuously change. In the case of $g_{12} = 5$, we see that they do not pass through each other. The two solitons change their shapes when they collide, and then almost recover to the original shapes after collision.

The problem whether the two wave packets would pass through each other is also

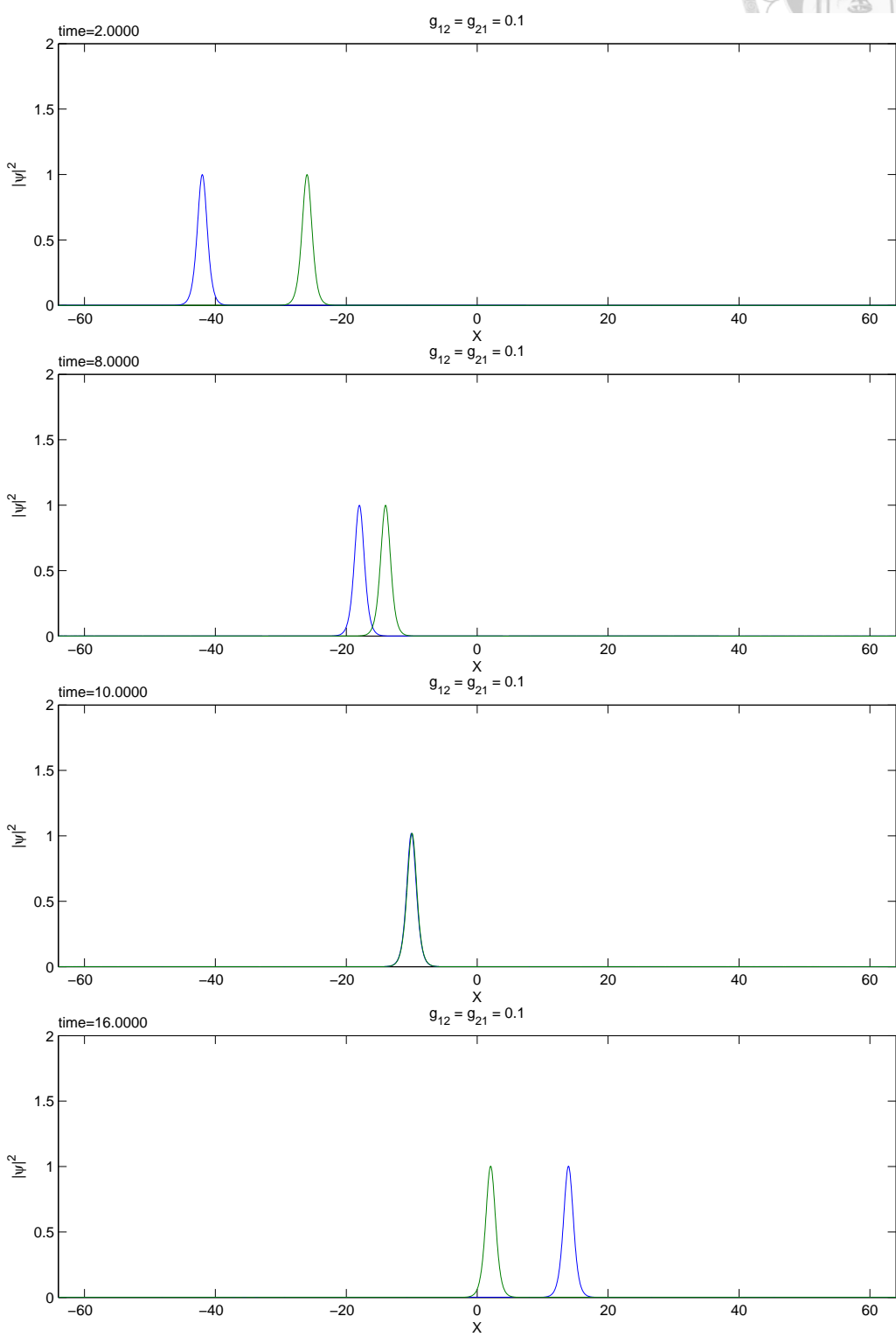
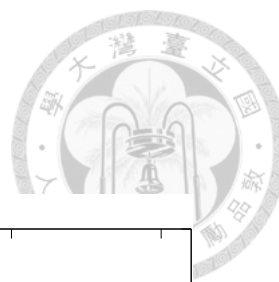


Figure 4.16: Density profiles of ψ_1 and ψ_2 at different time for $g_{12} = 0.1$ (example 3)

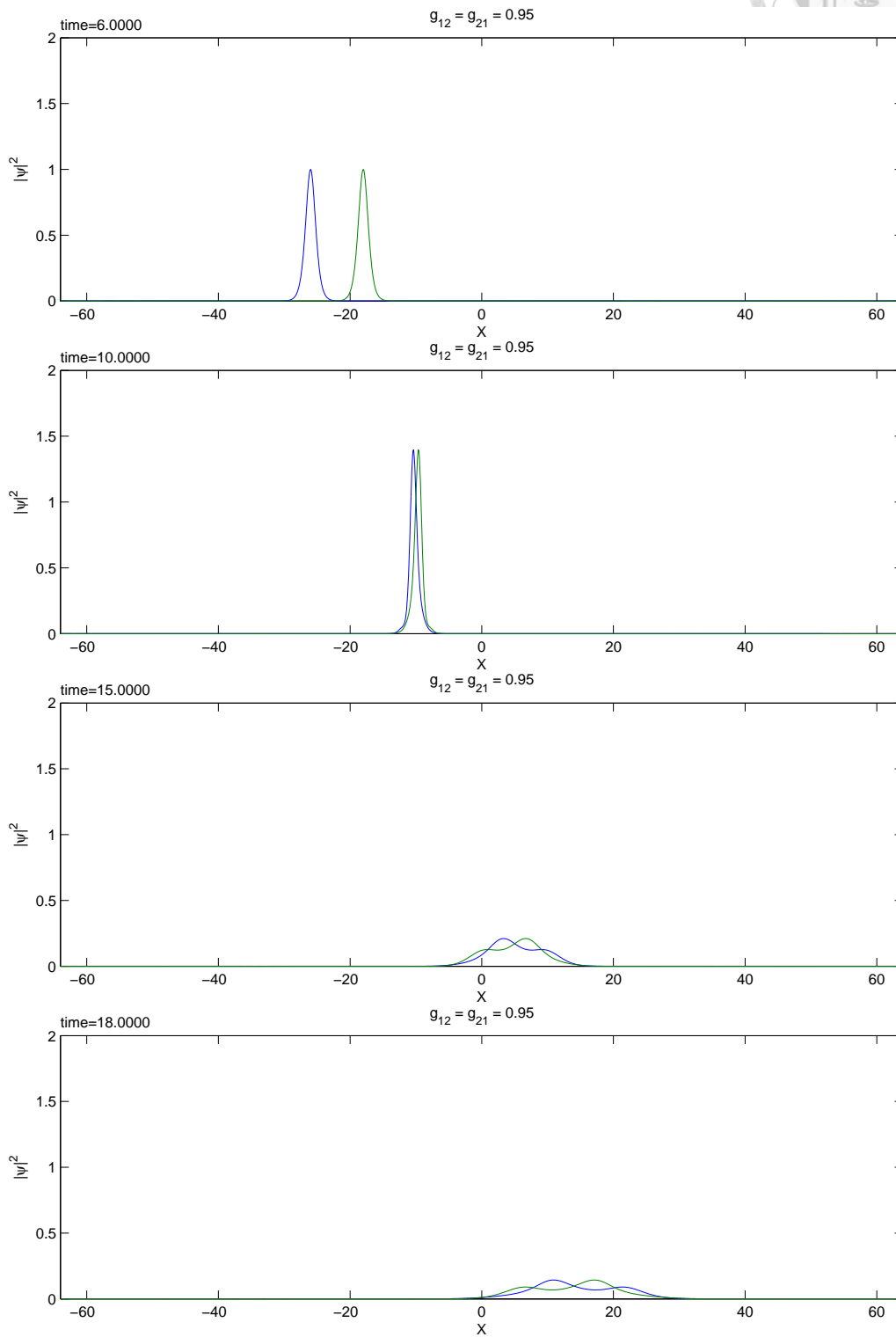
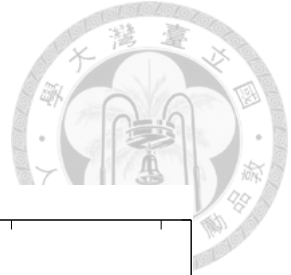


Figure 4.17: Density profiles of ψ_1 and ψ_2 at different time for $g_{12} = 0.95$ (example 3)

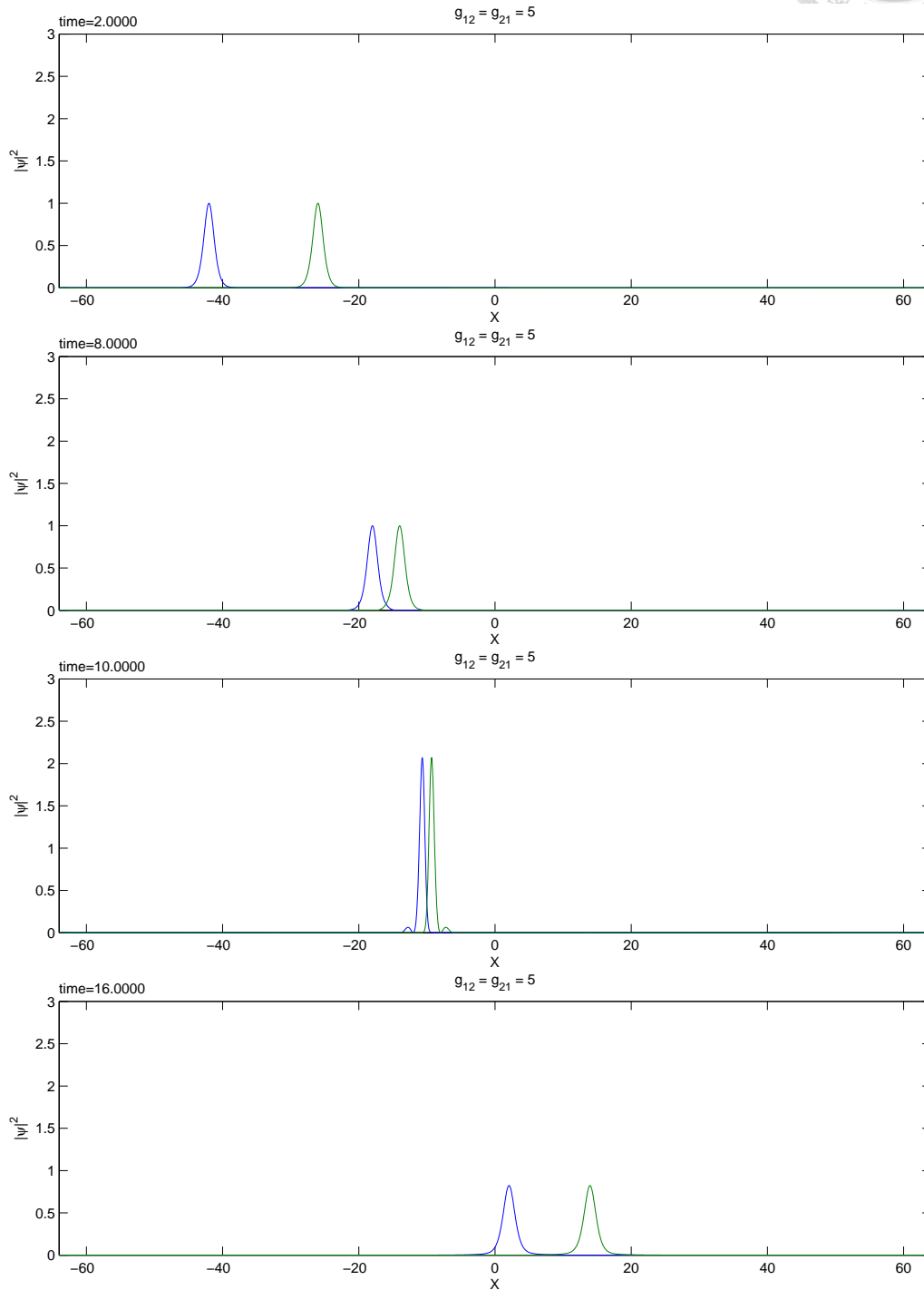


Figure 4.18: Density profiles of ψ_1 and ψ_2 at different time for $g_{12} = 5$ (example 3)

related to the initial kinetic energy for center of mass ($\frac{1}{2}N|\langle v \rangle|^2$). If the initial kinetic energy for center of mass of soliton 1 is large enough, then the repulsive force can not stop it during the interaction even when g_{12} is relatively large.

Next we observe the center of velocities vs. time graph for different values of g_{12} , shown in Figure 4.19. We see that when the interaction is weak, the center of velocity of ϕ_1 decrease and then increase during the collision. While the variation of the center of velocity of ψ_2 is reverse. This is similar to the attractive cases, but the interactive forces between waves are in opposite direction.

However, when the repulsive interactions are stronger, not the whole wave packets are able to pass through the other component. Thus the center of velocity of ψ_1 decreases and the center of velocity of ψ_2 increases after collisions. We observe that the momentum transfer is greater as the value of g_{12} is greater. When g_{12} is large enough, the two wave packets almost interchange their center of velocities after collisions, see Figure 4.20.

We say that the collision is like an elastic collision under strong repulsive interactions, in the following senses: 1. The waves do not pass through each other, and their fields almost do not overlap. 2. The kinetic energy for center of mass $\frac{1}{2}N\langle v \rangle_1^2 + \frac{1}{2}N\langle v \rangle_2^2$ is conserved after collisions.

Example 4: Solitons collision in 2D

In example 4 we solve the initial value problem in 2D. The initial conditions are taken as

$$\begin{aligned}\psi_1(x, 0) &= \phi(x - (-10, -5)) e^{i((2,1)\cdot x)}, \\ \psi_2(x, 0) &= \phi(x - (10, 5)) e^{i((-2,-1)\cdot x)}.\end{aligned}$$

The center of mass of soliton 1 and 2 are at $(-10, -5)$ and $(10, 5)$, respectively. The center of velocities of soliton 1 and 2 are $(2, 1)$ and $(-2, -1)$, respectively. They collide in

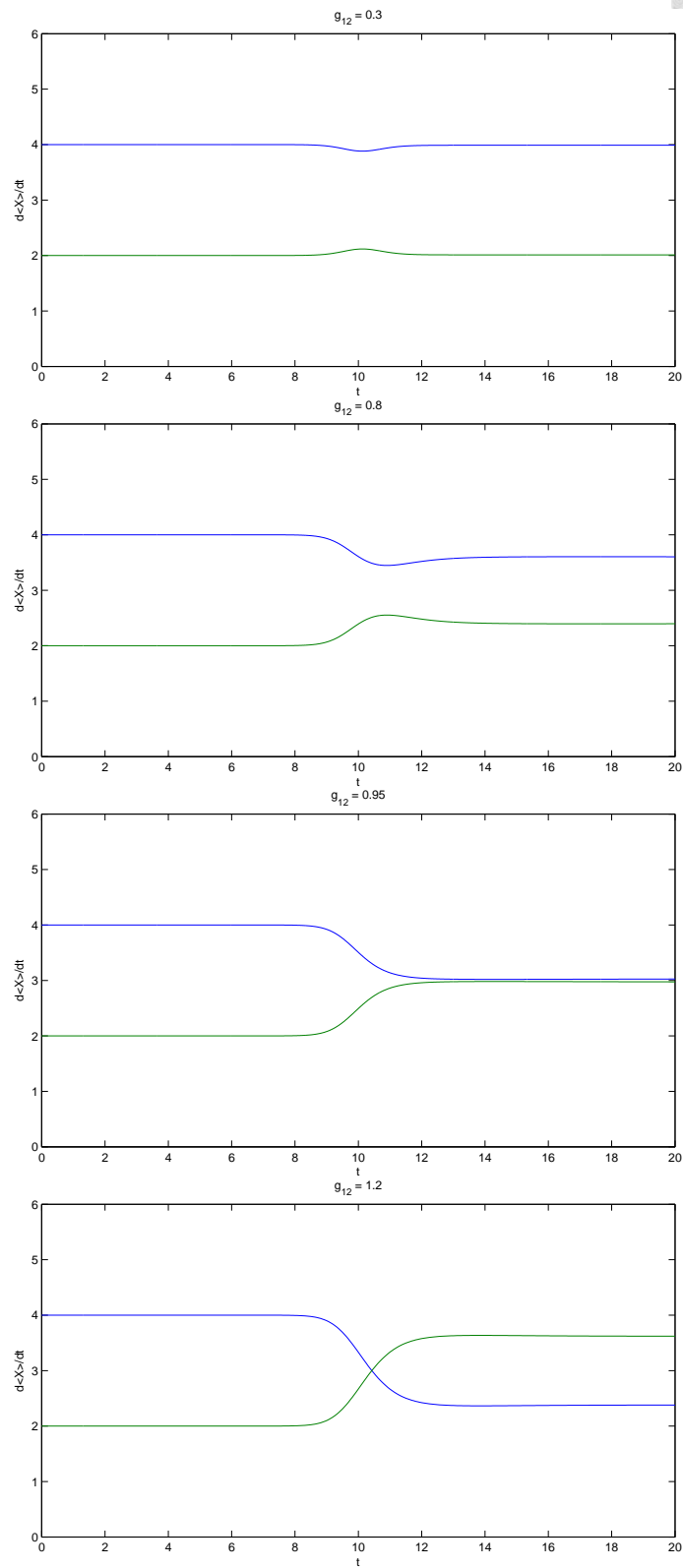
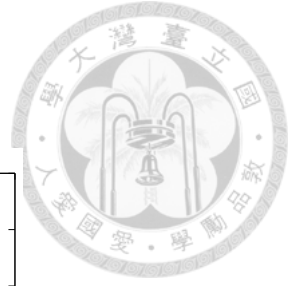


Figure 4.19: Velocity v.s. time graph for different values of g_{12} (example 3)

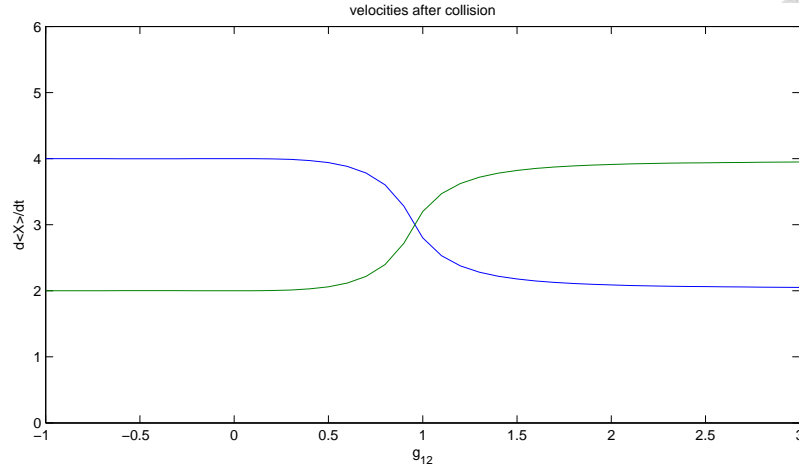
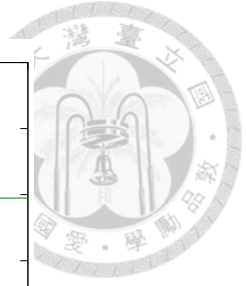


Figure 4.20: Velocities of the two wave packets after collisions with different values of g_{12} (example 3)

opposite direction. The density function of the initial conditions are shown in Figure 4.21.

We solve this initial value problem on $\Omega = (-64, 64)^2$ and choose the mesh $h = 1/16$

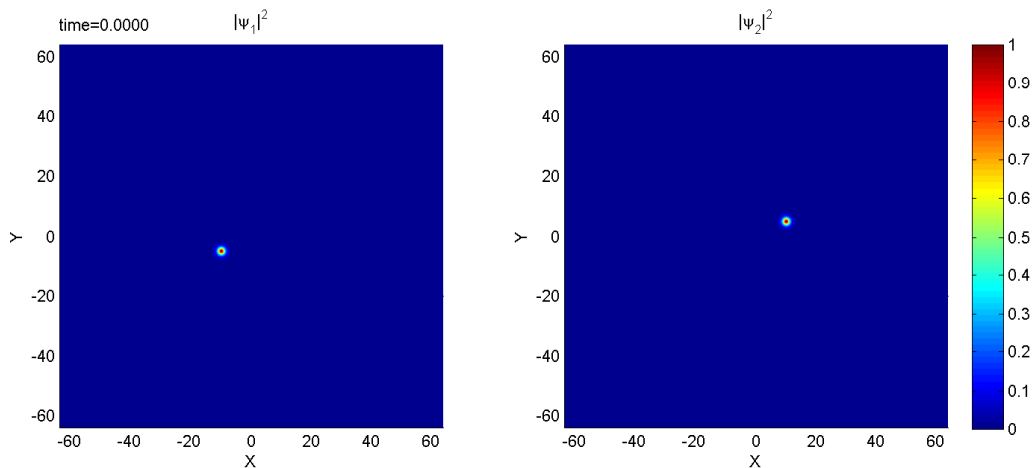


Figure 4.21: Initial conditions in example 4

and time step $\tau = 1/1024$.

1. Repulsive ($g_{12} = g_{21} > 0$)

We first observe the results under repulsive interactions between wave packets. Figure 4.22 shows the density profile of the two wave packets for $g_{12} = 2$ at different times. We see that the wave packets pass through each other, and then continuously spread out after the collision.

When the repulsive interactions are stronger, part of the wave packets reflect back

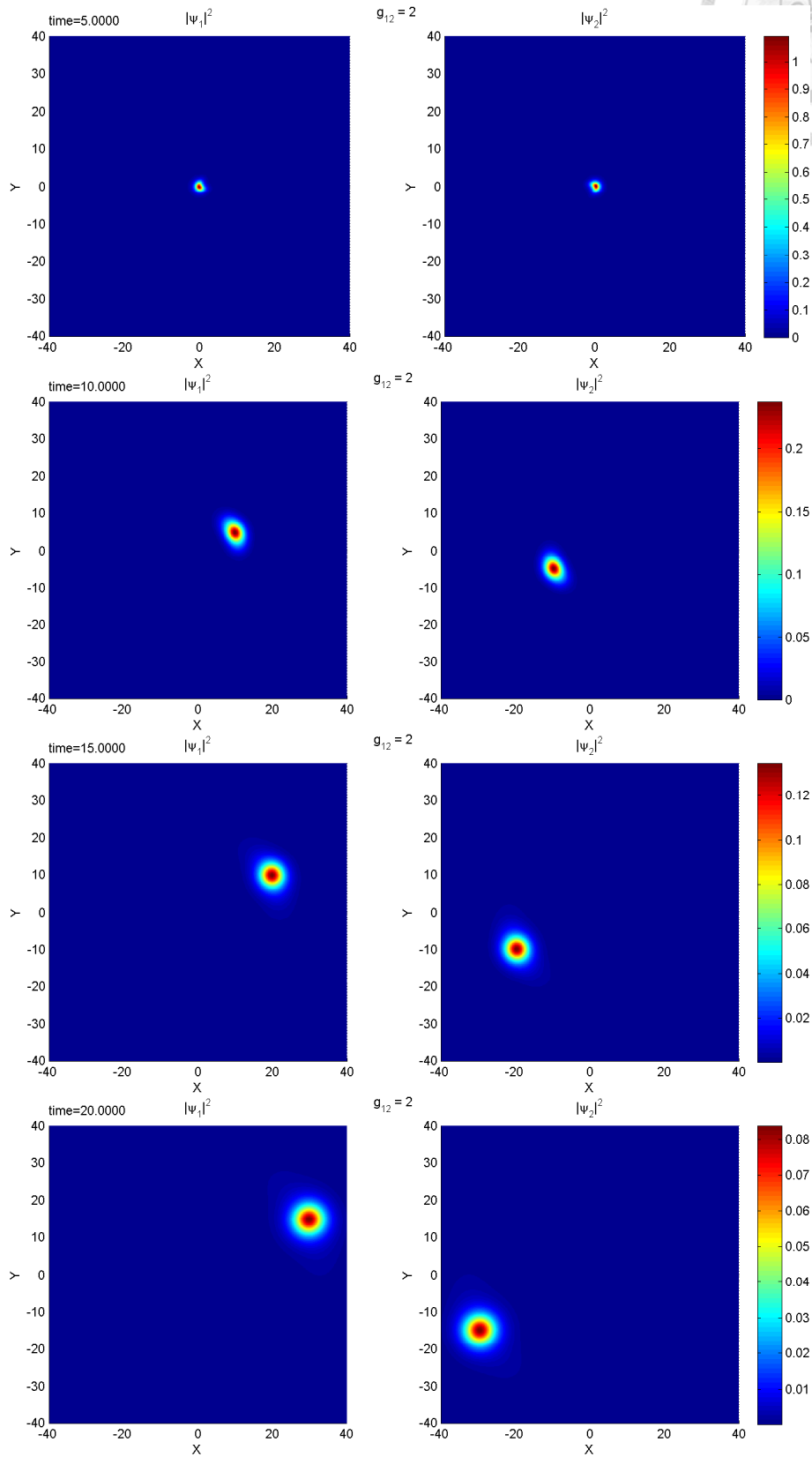
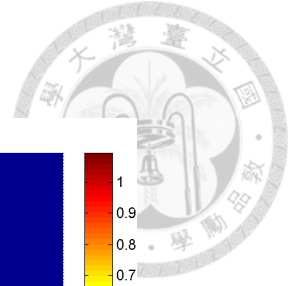


Figure 4.22: Density profiles of ψ_1 and ψ_2 at different time for $g_{12} = 2$ (example 4)

after collisions. Figure 4.23 shows the density profiles of the two components at different time for $g_{12} = 4$. We see that after the collision, part of the waves reflect back in the direction they came from and the other part continue to move forward. The latter part splits into two groups separated by the reflected wave of the other component.

Figure 4.24 shows the density profiles of the two components at different time for $g_{12} = 6$. We see that most of the waves reflect back after collision.

We find that all the waves in these cases spread out after collisions. For those cases in which waves are separated into parts after collisions, this is expected since the mass of the wave packets are less than the mass of solitons in 2D. For the other cases, we can check the results by verifying the variance identity. First we observe the absolute value of the center of velocities $|\langle v \rangle|$ vs. time graph. The graphs for $g_{12} = 1, 2, 3$ are shown in Figure 4.25.

We see that the speeds of center of mass decrease after collisions. Thus the internal kinetic energy $KE_{int} = E - \frac{1}{2}N|\langle v \rangle|^2$ after collisions are greater than their initial values. Since the initial internal kinetic energy is zero, we get that $KE_{int} > 0$ after collisions. Hence by the variance identity, the width of the waves w grows quadratically with time after collisions, meaning that the wave packets spread out.

Figure 4.26 shows the width w_1 of ψ_1 vs. time graph for $g_{12} = 2$ during $t = 8 \sim 20$ (after the collision). The fitting curve on the graph is a quadratic curve with a positive quadratic coefficient as we expect. The differences between the quadratic coefficients and the internal kinetic energy after is $1.178E-2$.

2. Attractive ($g_{12} = g_{21} \leq 0$)

We first observe the results for $g_{12} = -1$. The profile of the density functions $|\psi|^2$ at different time are shown in Figure 4.27. We see that the waves grow up and then continuously decay after collision.

For attractive interaction between waves, we discuss two things: 1. Whether all the wave packets eventually decay? 2. Would the wave packets blow up during

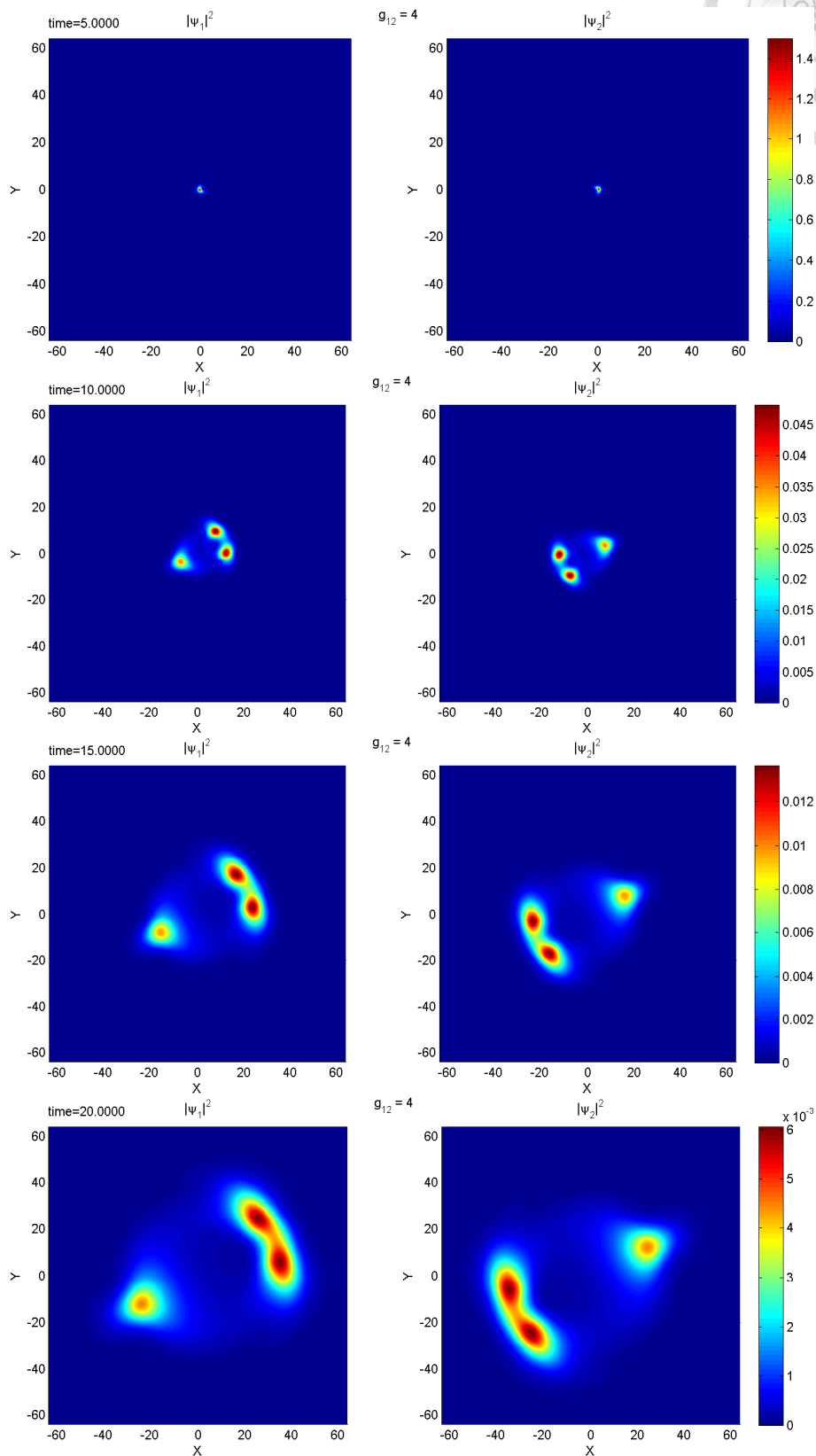
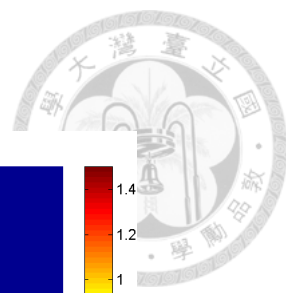


Figure 4.23: Density profiles of ψ_1 and ψ_2 at different time for $g_{12} = 4$ (example 4)

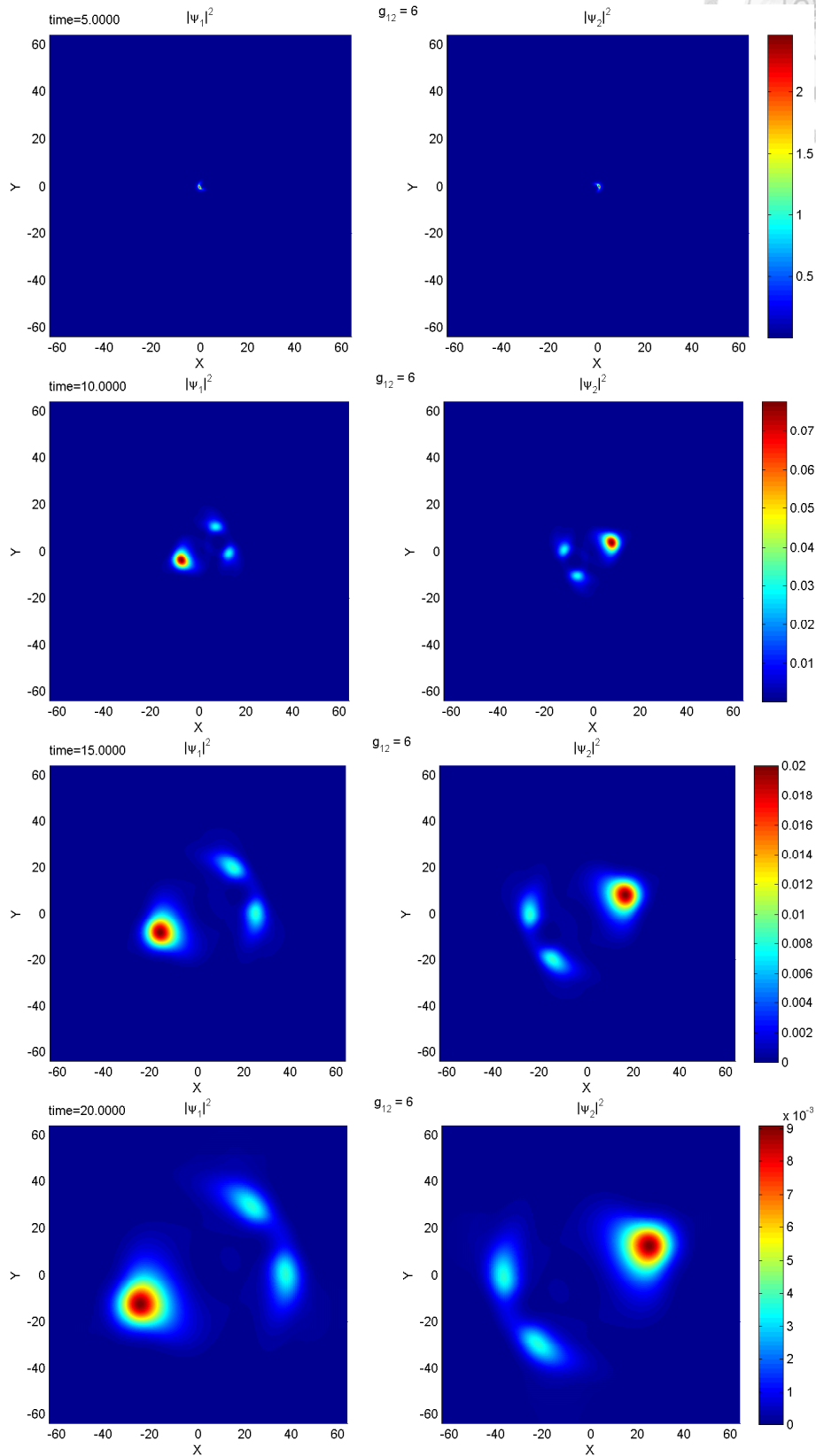
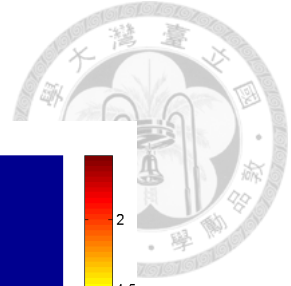


Figure 4.24: Density profiles of ψ_1 and ψ_2 at different time for $g_{12} = 6$ (example 4)

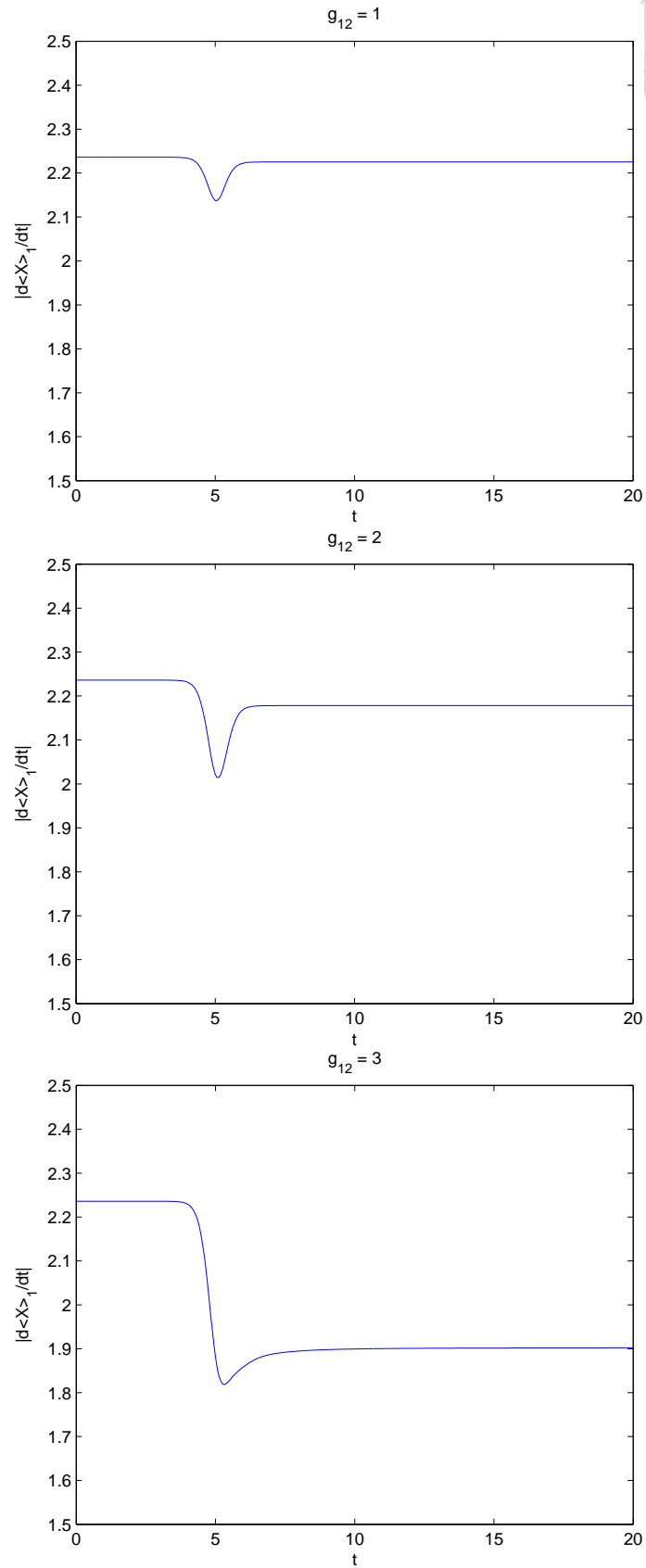
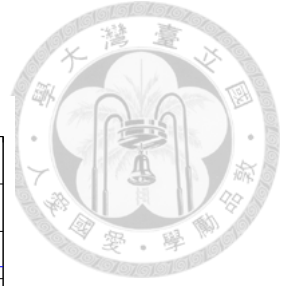


Figure 4.25: $|\langle v \rangle|$ v.s. time with different values of g_{12} (example 4)

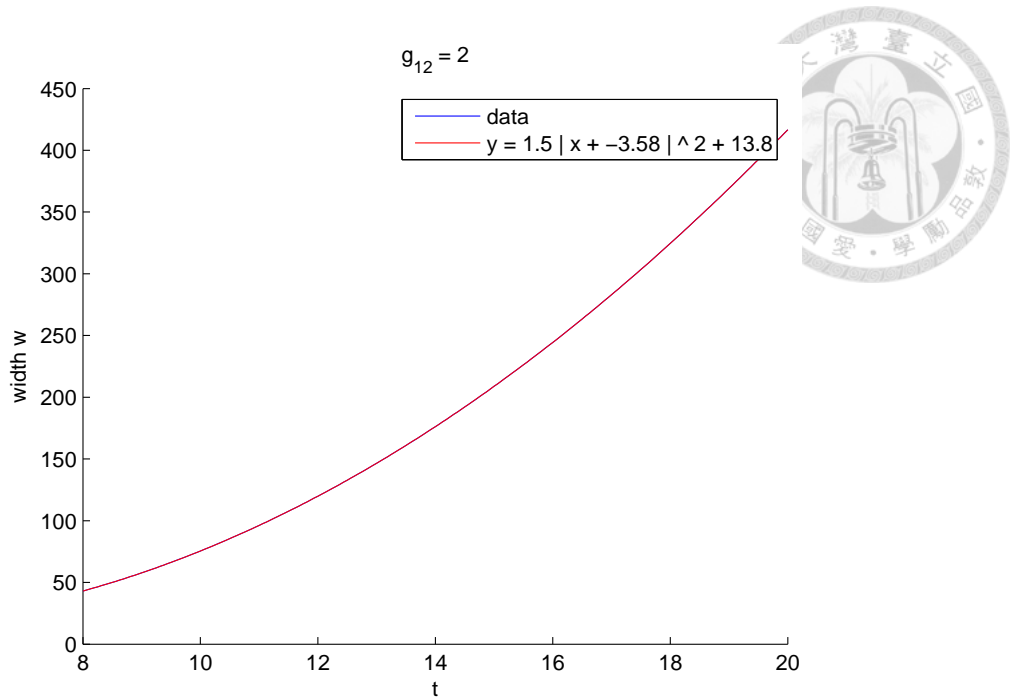


Figure 4.26: w v.s. time graph after collision for $g_{12} = 2$ (example 4)

collisions when the attractive interactions between them are strong enough?

To answer the first question, we observe the speed of the center of mass $|\langle v \rangle|$ vs. time graph. The graph for $g_{12} = -1, -2, -3, -4$ are shown in Figure 4.28. We see that the speeds after collisions are lower than their initial values (and the values are lower for lower g_{12}). Hence, as previously discussed, the internal kinetic energies of the two wave packets are positive after collisions. The wave packets would then spread out.

For the second question, we need a criteria to judge whether a solution blows up. Here we can not use the variance identity, since it is for single GPE and the interactions during collisions can not be neglected. (In fact the positive width still does not imply the global existence of the solution.) We judge whether solutions blow up only by checking whether the energy is conserved.

Let us observe the results of soliton collisions under stronger attractive interactions. We set the mesh size $h = 1/32$ for $g_{12} < -5$. As we lower the value of g_{12} , we find that the energy is not conserved during collision when $g_{12} = -6$. The density profile of the waves at different time are shown in Figure 4.29 and Figure 4.30. We see that the two wave packets pass through each other at first, but then they

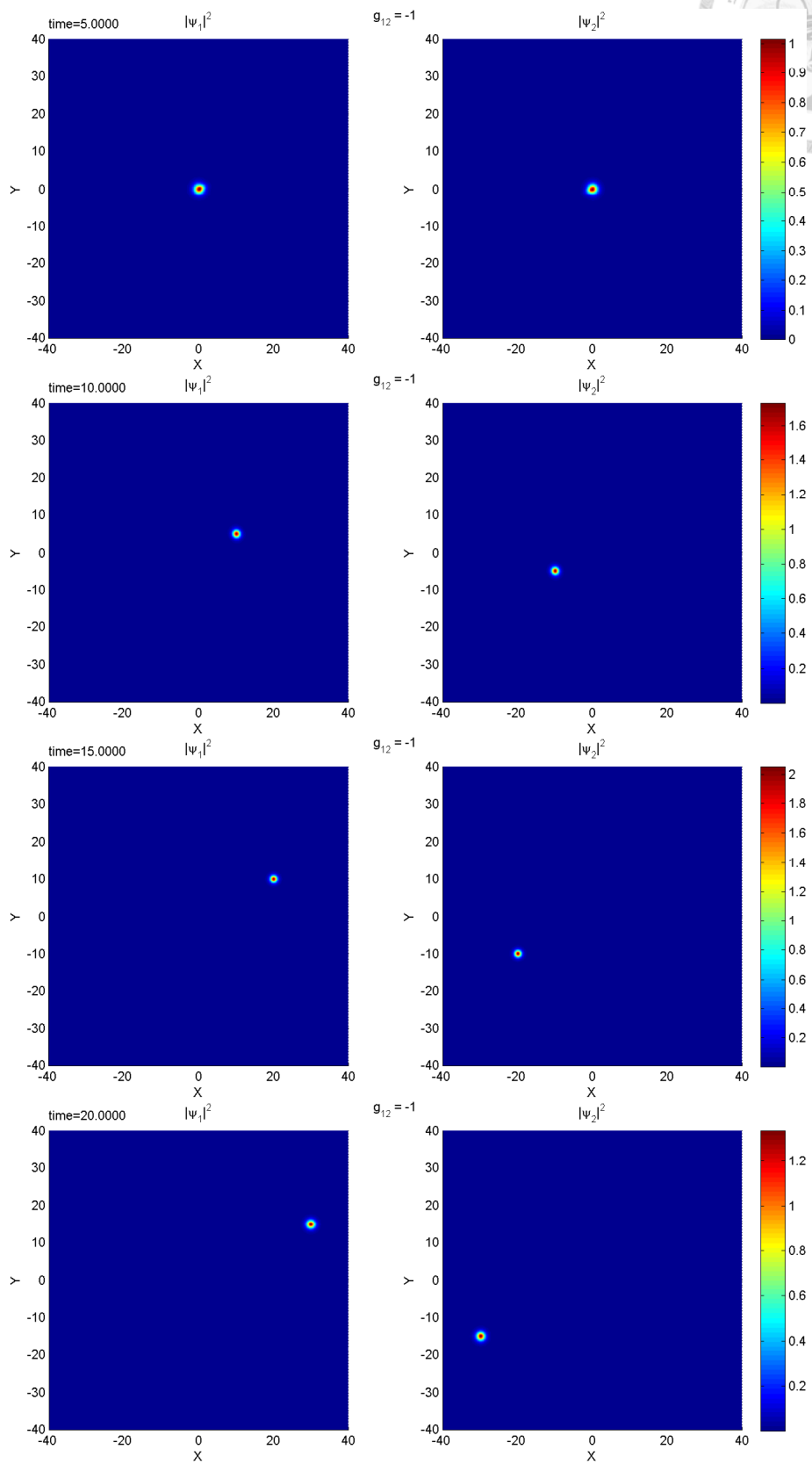
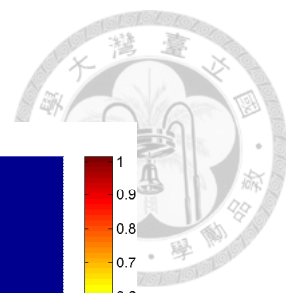


Figure 4.27: Density profiles of ψ_1 and ψ_2 at different time for $g_{12} = -1$ (example 4)

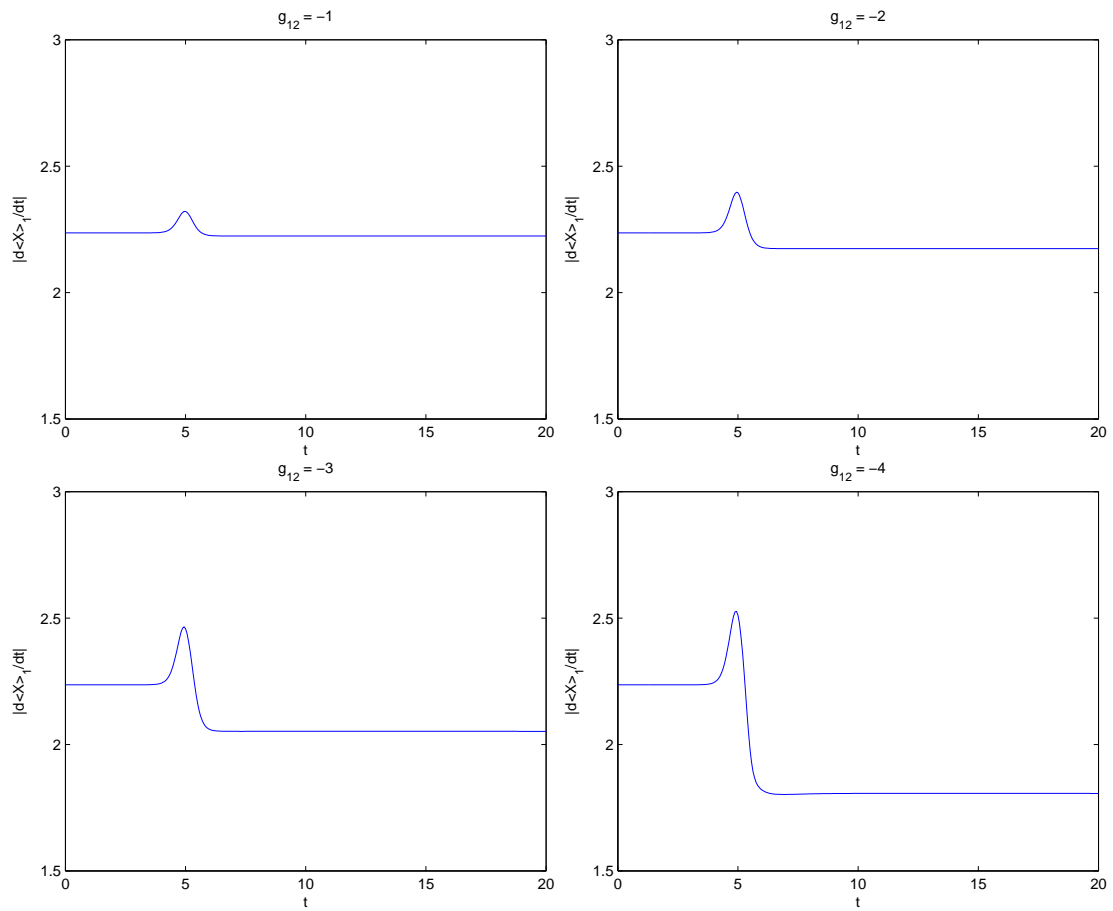


Figure 4.28: $|d\langle x \rangle_1/dt|$ v.s. time with different values of g_{12} (example 4)

are pulled back together by the attractive force and their amplitude grow up. The energy vs. time graph is shown in Figure 4.31. The energies are not conserved near the time $t \approx 5.78$.

The waves can blow up in a shorter time when the attractive interactions are even stronger, see the case for $g_{12} = -8$ shown in Figure 4.32. The energy vs. time graph for $g_{12} = -8$ is shown in Figure 4.33, the energy is not conserved near the time $t \approx 5.33$.

In these two cases we know that the wave packets would blow up during collision when the attractive interactions between them are strong enough.

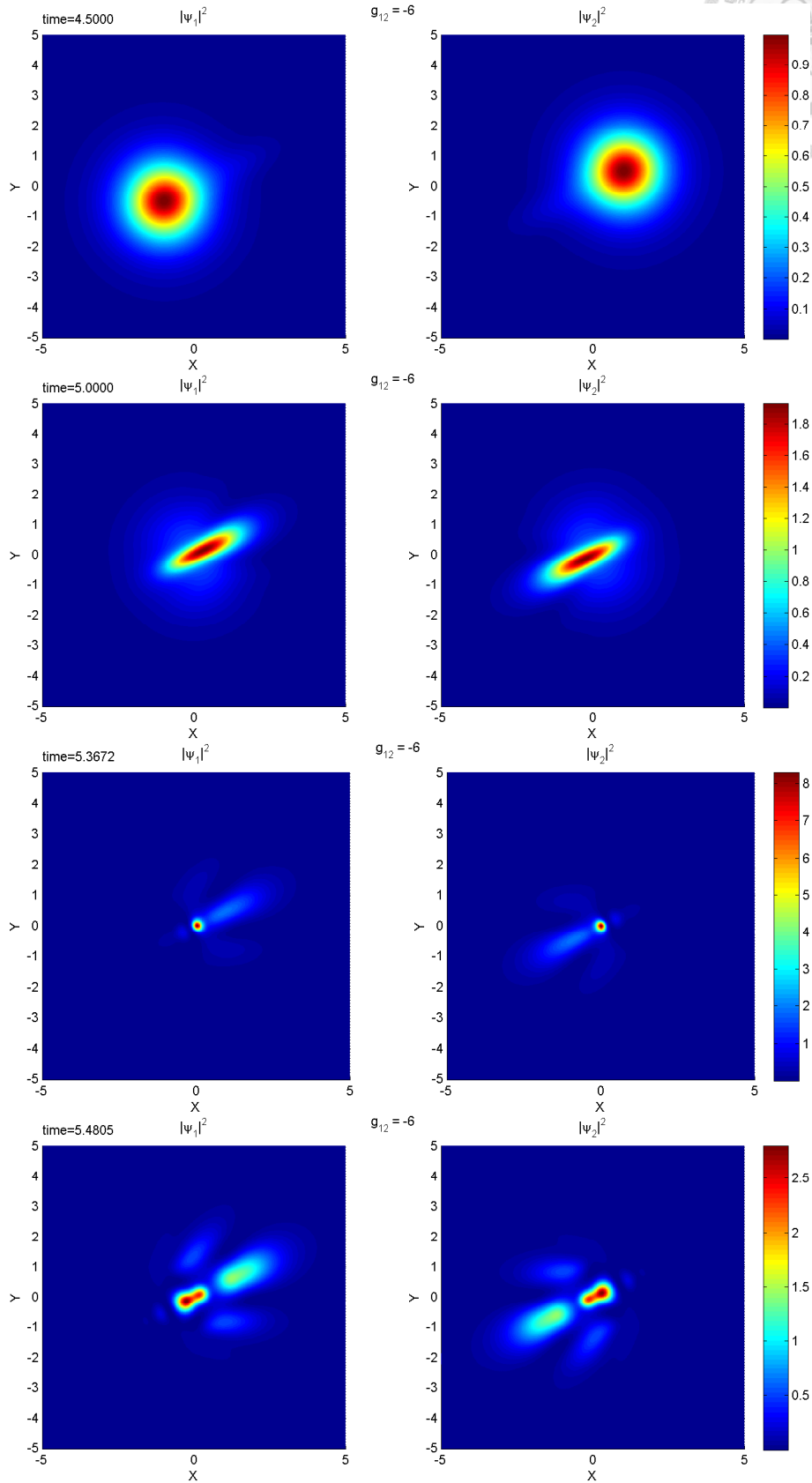
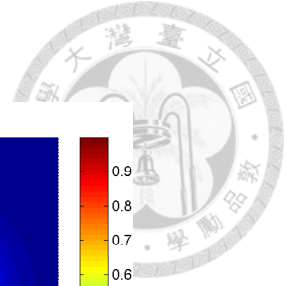


Figure 4.29: Density profiles of ψ_1 and ψ_2 at different time for $g_{12} = -6$ (example 4)

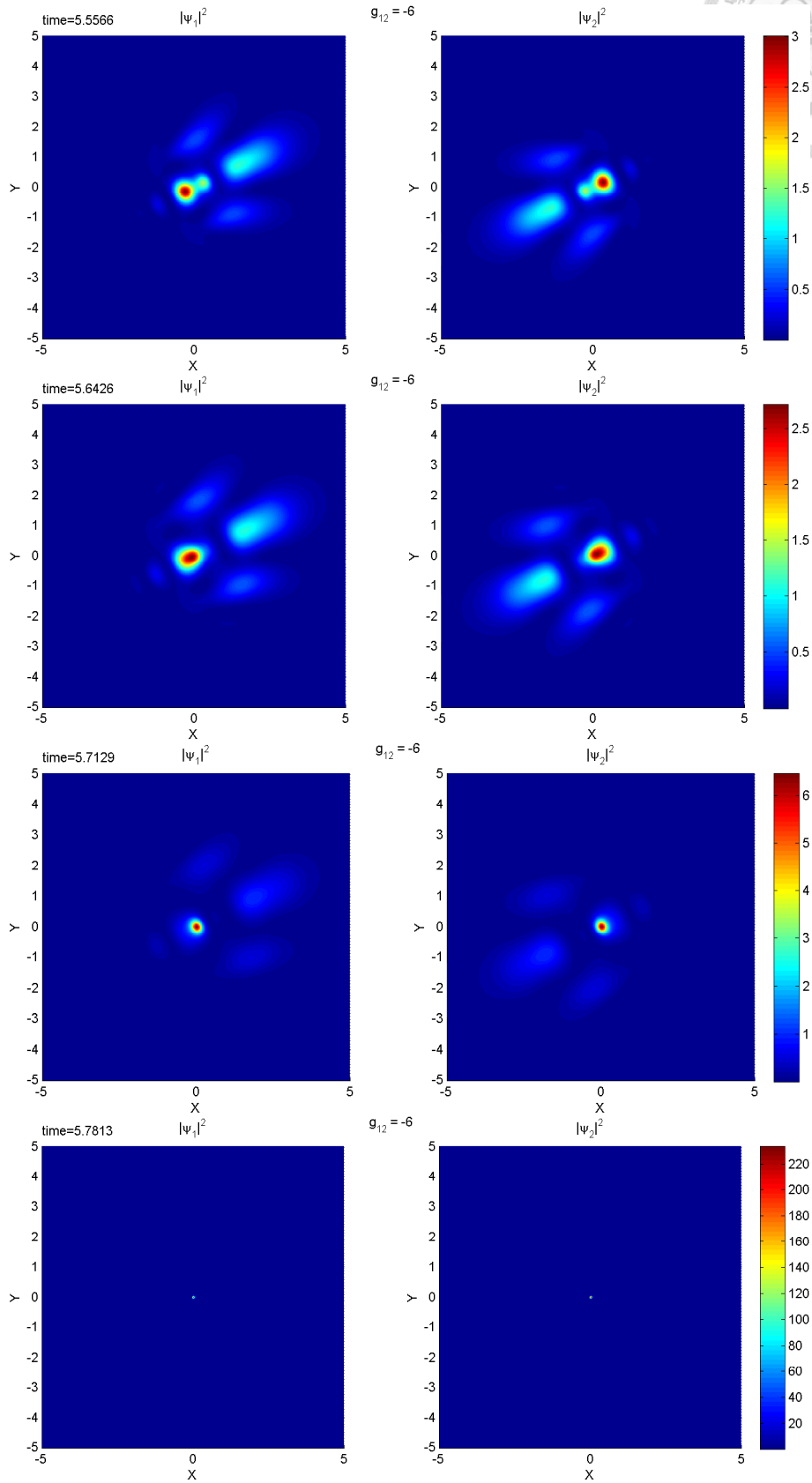
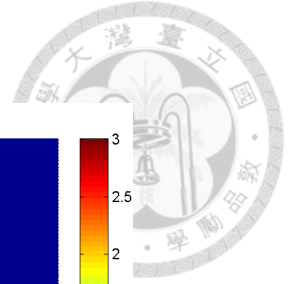


Figure 4.30: Density profiles of ψ_1 and ψ_2 at different time for $g_{12} = -6$ (2) (example 4)

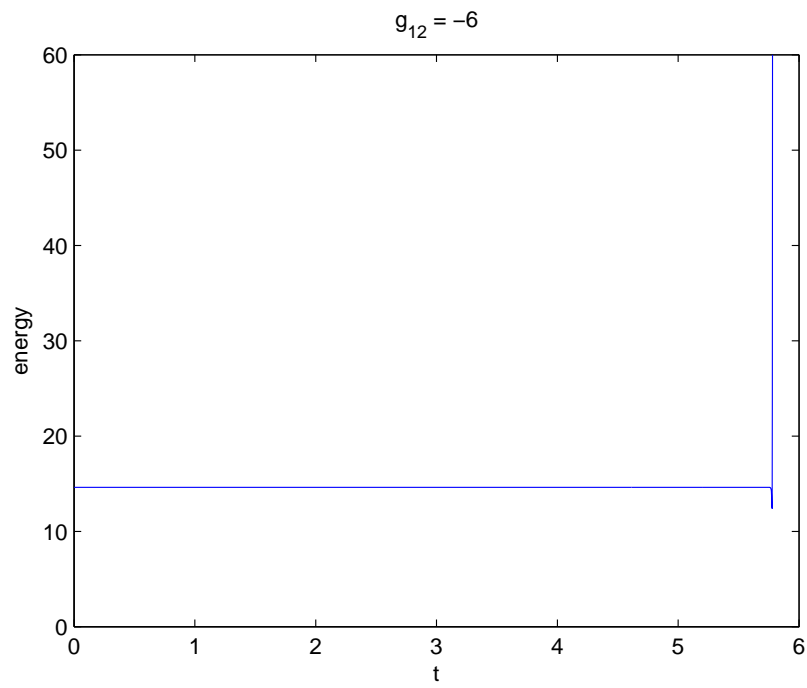


Figure 4.31: Energy v.s. time graph for $g_{12} = -6$

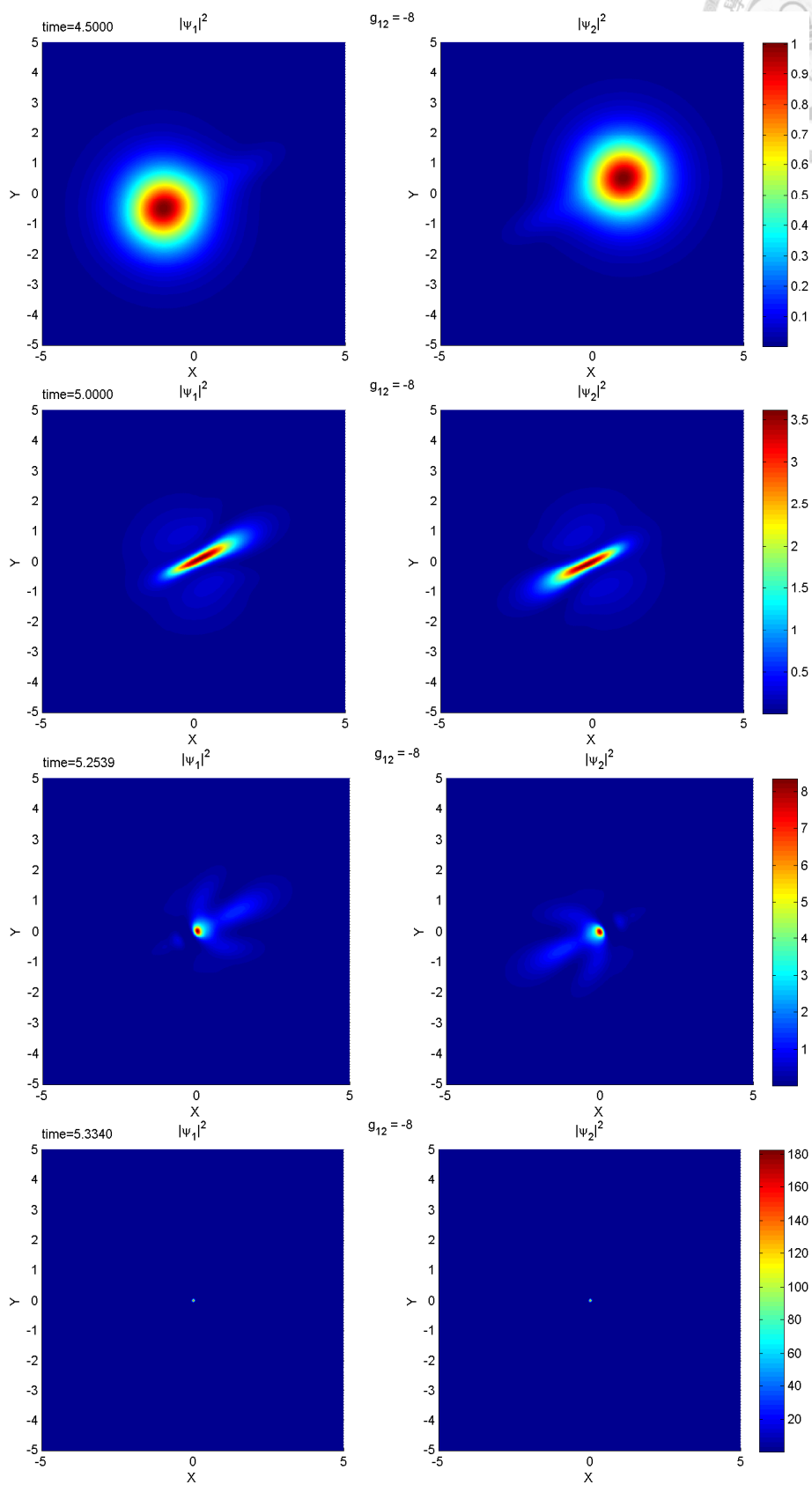
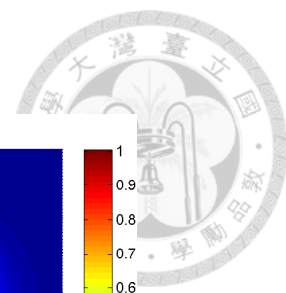


Figure 4.32: Density profiles of ψ_1 and ψ_2 at different time for $g_{12} = -8$ (example 4)

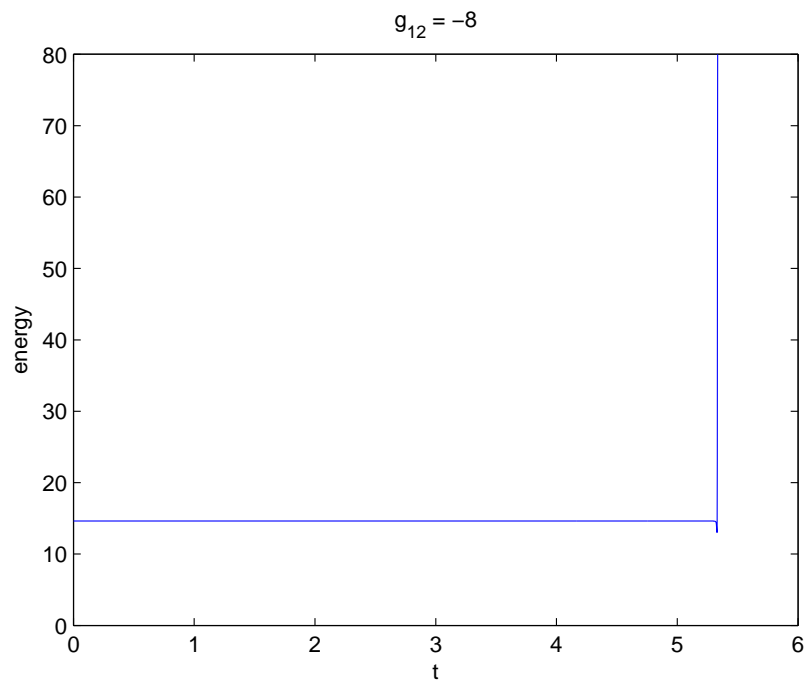


Figure 4.33: Energy v.s. time graph for $g_{12} = -8$ (example 4)



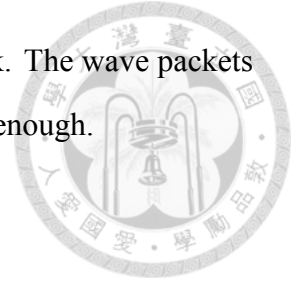
5. Conclusions

We investigate interactions of bright solitons in two-component BECs. The numerical results are basically consistent with the one-component theoretical results that solitons are stable in 1D and unstable in 2D.

We perform collision of two solitons belonging to different component. We outline the results as follows.

1. 1D, repulsive interactions between two species: the collisions are inelastic when the interactions are weak, in the sense that the waves do not completely separate after the collisions. The collisions are like elastic collisions when the repulsive interactions are strong, in the senses that (1) they completely separate and keep their shapes almost intact after collisions. (2) The kinetic energy for center of mass of the two wave packets is conserved.
2. 1D, attractive interactions between two species: solitons pass through each other. For weak interactions, the speeds of solitons change during collisions and hence cause the position shifts. For strong interactions, after the collisions there are small waves separated from the original solitons which follow the waves of the other component.
3. 2D, repulsive interactions between two species: all the waves spread out after collisions. When the interactions are weak, the wave packets pass through each other. When the interactions are stronger, part of the wave reflect back and the other part split into two groups and continue to move forward.
4. 2D, attractive interactions between two species: the wave packets pass through each

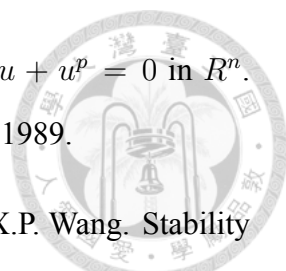
other and eventually spread out when the interactions are weak. The wave packets blow up during the collisions when the interactions are strong enough.





References

- [1] Weizhu Bao and Yongyong Cai. Mathematical theory and numerical methods for Bose-Einstein condensation. *Kinetic & Related Models*, 6(1), 2013.
- [2] Weizhu Bao, I-Liang Chern, and Fong Yin Lim. Efficient and spectrally accurate numerical methods for computing ground and first excited states in Bose-Einstein condensates. *Journal of Computational Physics*, 219(2):836–854, 2006.
- [3] R Carretero-González, DJ Frantzeskakis, and PG Kevrekidis. Nonlinear waves in Bose-Einstein condensates: physical relevance and mathematical techniques. *Nonlinearity*, 21(7):R139, 2008.
- [4] T. Cazenave and P.-L. Lions. Orbital stability of standing waves for some nonlinear Schrödinger equations. *Comm. Math. Phys.*, 85(4):549–561, 1982.
- [5] Franco Dalfovo, Stefano Giorgini, Lev P. Pitaevskii, and Sandro Stringari. Theory of Bose-Einstein condensation in trapped gases. *Rev. Mod. Phys.*, 71:463–512, Apr 1999.
- [6] L.C. Evans. *Partial Differential Equations*. Graduate studies in mathematics. American Mathematical Society, 1998.
- [7] GM Fraiman. The asymptotic stability of the manifold of self-similar solutions in the presence of self-focusing. *Zhurnal Eksperimentalnoi i Teoreticheskoi Fiziki*, 88:390–400, 1985.
- [8] R. T. Glassey. On the blowing up of solutions to the cauchy problem for nonlinear Schrödinger equations. *Journal of Mathematical Physics*, 18(9):1794–1797, 1977.

- 
- [9] ManKam Kwong. Uniqueness of positive solutions of $\Delta u - u + u^p = 0$ in R^n . *Archive for Rational Mechanics and Analysis*, 105(3):243–266, 1989.
- [10] M.J. Landman, G.C. Papanicolaou, C. Sulem, P.L. Sulem, and X.P. Wang. Stability of isotropic singularities for the nonlinear Schrödinger equation. *Physica D: Nonlinear Phenomena*, 47(3):393 – 415, 1991.
- [11] C. Sulem and P.L. Sulem. *The Nonlinear Schrödinger Equation: Self-Focusing and Wave Collapse*. Number 139 in Applied Mathematical Sciences. Springer, 1999.
- [12] Terence Tao. Why are solitons stable? *Bulletin of the American Mathematical Society*, 46(1):1–33, 2009.
- [13] Michael I. Weinstein. Nonlinear Schrödinger equations and sharp interpolation estimates. *Communications in Mathematical Physics*, 87(4):567–576, 1982.